Int J Earth Sci (Geol Rundsch) (2011) 100:489–510
DOI 10.1007/s00531-010-0584-4

ORIGINAL PAPER

Neoproterozoic to Lower Palaeozoic successions of the Tandilia System in Argentina: implication for the palaeotectonic framework of southwest Gondwana

Udo Zimmermann · Daniel G. Poiré · Lucía Gómez Peral

Received: 9 November 2009 / Accepted: 28 June 2010 / Published online: 28 August 2010

Abstract The Cryogenian to Uppermost Ediacaran successions of the Tandilia System (Sierras Bayas Group and Cerro Negro Formation) in central-eastern Argentina is exceptional because of its unmetamorphosed and nearly undeformed character, its sediment provenance trend and the absence of any identified glacial deposit and the deposition of warm water carbonates. We decipher a dramatic change in the basin evolution from small-scale depositional areas during the Neoproterozoic to a larger basin related to an active continental margin throughout the Uppermost Ediacaran. The base of the succession is represented by immature detritus of alkaline composition (Villa Mónica Formation), but towards the top of this formation, the material is sorted and reworked, nonetheless still reflecting in its detritus the local rocks. The clastic deposition is interrupted by diagenetic overprinted dolomites. The unconformable overlying quartz-arenitic Ediacaran Cerro Largo Formation reworked the Cryogenian Villa Mónica Formation and contains mainly felsic granitic and metamorphic basement material of slightly wider variety, while the dominant alkaline geochemical signature in rocks of the Villa Mónica Formation disappears. Based on diagenetic, petrographic and sedimentological data, we can interpret the unconformity representing a longer time of erosion. The Cerro Largo Formation shows a transition to mudstones and the heterolithic facies of the Olavarría Formation. The top of the Sierras Bayas Group is represented by limestones (Loma Negra Formation), which are discordantly overlain by the Uppermost Ediacaran Cerro Negro Formation. The latter displays detrital material derived from a continental arc, mafic and felsic sources. Several arc-related geochemical proxies ($Th/Sc < 0.8$; $Zr/Sc < 10$; $La/Sc < 2$; $Ti/Zr > 20$) are recorded in the sediment detritus, as are syn-depositional pyroclastites. The absence of volcanic material in the underlying rocks allows proposing that the Cerro Negro Formation is related to an active continental margin fringing Gondwana ("Terra Australis Orogen") as a retro-arc or retro-arc foreland basin.

Keywords Neoproterozoic · Lower Palaeozoic · SW Gondwana · Provenance study · Eastern Argentina · Active continental margin

Electronic supplementary material The online version of this article (doi:10.1007/s00531-010-0584-4) contains supplementary material, which is available to authorized users.

U. Zimmermann (✉)
Department of Petroleum Engineering,
University of Stavanger, 4036 Stavanger, Norway
e-mail: udo.zimmermann@uis.no

U. Zimmermann
Department of Geology, University of Johannesburg,
Johannesburg, South Africa

D. G. Poiré · L. G. Peral
Centro de Investigaciones Geológicas (CONICET-Universidad Nacional de La Plata), Calle 1 no 644,
B1900TAC La Plata, Argentina

Introduction

Neoproterozoic successions in the Tandilia System in Argentina (Fig. 1) are well characterised in terms of petrography and sedimentary facies (Poiré 1987, 1993; Gómez Peral et al. 2007). However, the exact age and tectonic setting are not perfectly constrained. In the context of the "snowball earth hypothesis" and the palaeotectonic evolution of SW Gondwana with its numerous Neoproterozoic to Lower Palaeozoic basins (Fig. 1b), this

succession is exceptional as the rocks are nearly undeformed, unmetamorphosed and void of clastic glacial deposits as well as so-called cap carbonates or Fe-rich deposits (Poiré 1987, 2004; Gómez Peral et al. 2007; Zimmermann 2009; Van Staden et al. 2010).

The objective of this study is to decipher the composition of the clastic sedimentary rocks to gain insight into the basin evolution in southwest Gondwana. Provenance characteristics will point out changes in the sedimentary sources and combined with the possible transport mechanisms of the involved detritus allow in developing a basin model. We present here detailed petrographic and chemostratigraphic data of the Neoproterozoic Sierras Bayas Group and the overlying Cerro Negro Formation and will merge the data with recently published regional provenance information and palaeotectonic models. This will demonstrate that large-scale regional models still refrain from substantial proofs, as the geological evolution seems to be more complicated than assumed.

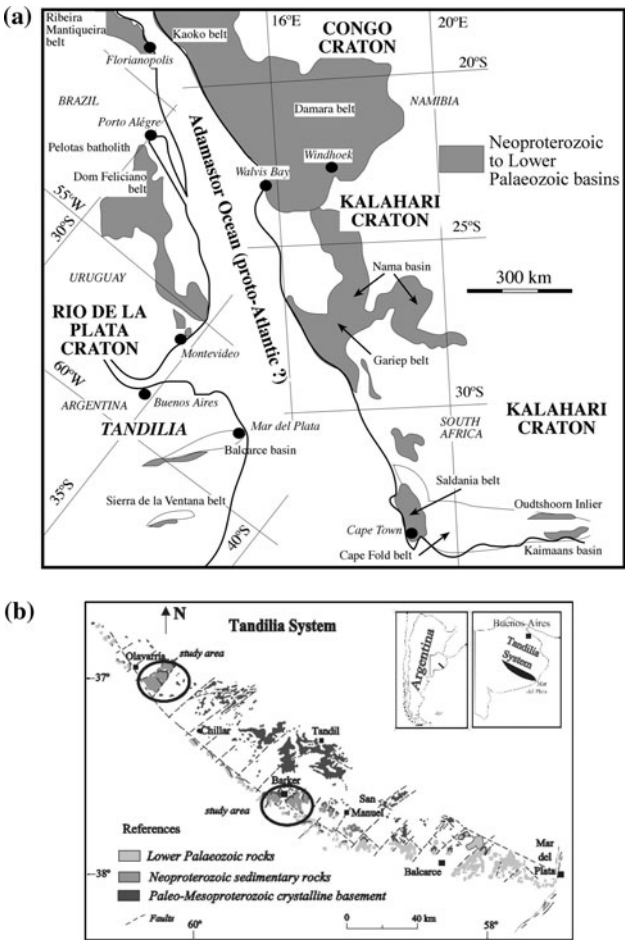

Fig. 1 **a** Palaeogeographic setting of different Neoproterozoic successions (after Rapela et al. 2003). **b** Geological map of the Tandilia System and sampling locations (after Gómez Peral et al. 2007)

Geology and stratigraphy

The Tandilia System is a 350 km long, northwest southeast oriented orographic belt, located in the Buenos Aires province in Argentina (Fig. 1). It comprises an igneous-metamorphic basement covered by Neoproterozoic to Lower Palaeozoic sedimentary rocks (Fig. 2a). The basement rocks are mainly granitoids, orthogneisses and migmatites yielding Sm–Nd model ages averaging 2,620 ± 80 Ma and detrital zircons pointing to Archaean sources for Neoproterozoic and Lower Palaeozoic successions (Pankhurst et al. 2003; Rapela et al. 2007; Gaucher et al. 2008). In the Olavarría area (Fig. 1b), the Neoproterozoic succession is composed of the Villa Mónica (Fig. 2b), Cerro Largo (Fig. 2c), Olavarría and Loma Negra Formations (Sierras Bayas Group), with a thickness of ~170 m (Poiré 1993), covered by the Cerro Negro Formation (Fig. 2d). In other areas the Las Águilas Formation is considered as deposited between the Cerro Largo and Loma Negra Formation instead of the Olavarría Formation (Poiré and Spalletti 2005). The Cerro Negro Formation is overlain by the quartz-arenites, glacial diamictites and tuffs of the Balcarce Formation (Fig. 2e).

The lithostratigraphic units can be grouped into five depositional sequences (Fig. 2): Tofoletti (I), Malegni (II), Diamante (III), Villa Fortabat (IV) and La Providencia (V) (Spalletti and Poiré 2000; Poiré and Spalletti 2005). The different sequences reflect different depositional systems (see compilation in Poiré 1987; Spalletti and Poiré 2000; Poiré et al. 2003; Poiré and Spalletti 2005; Gómez Peral et al. 2007) from a shallow water environment with the occurrence of stromatolites (Tofoletti sequence, 52–70 m thick), to a basin margin facies with abundant cross-bedded quartz arenites overlain by thin layers of silt- and mudstones and thin beds of banded iron formation (Malegni sequence, 45 m). The Diamante depositional sequence (35 m) shows relatively similar facies conditions, with abundant mudstones and heterolithic facies. The Villa Fortabat (40 m) comprises almost exclusively limestones, originated by suspension fallout in open marine ramp and lagoonal environments. Diagenetic studies show that the C–O isotope systems are primary and may point to an Ediacaran age (Gómez Peral et al. 2007), which was substantiated by the finding of *Cloudina* sp. and latest Ediacaran acritarchs (Gaucher et al. 2005). The Sierras Bayas Group is overlain by the Cerro Negro Formation with an erosional unconformity (Barrio et al. 1991; Poiré et al 2007; Fig. 2). This surface has been related to eustatic sea-level drop and could be found in other eastern South American basins (Gaucher and Poiré 2009b). Meteoric dissolution of the carbonate sediments is interpreted as a karstic surface onto which residual clays and brecciated chert were deposited (Barrio et al. 1991; Gómez Peral et al. 2007).

(a)

Eras-Period	*Depositional Sequences*	Stratigraphic Units NW REGION		CENTRAL REGION		SE REGION
SILURIAN	Batán Sequence	Balcarce Formation		Balcarce Formation		Balcarce Formation
HIRNANTIAN						Sierra del Volcán diamictites
ORDOVICIAN						Balcarce Formation ?
CAMBRIAN	La Providencia Sequence	*Cerro Negro Formation* ?		*Cerro Negro Formation* ?		Punta Mogotes Formation
UPPER EDIACARAN (c. 580 Ma ?)	Villa Fortabat Sequence	Sierras Bayas Group	Loma Negra Formation	Sierras Bayas Group	Loma Negra Formation	
NEO-	Diamante Sequence		*Olavarría Formation*		*Las Aguilas Formation*	
PROTERO-	Malegni Sequence		*Cerro Largo Formation*		*Cerro Largo Formation*	
ZOIC (c. 800-900 Ma)	Tofoletti Sequence		*Villa Mónica Formation*		*Villa Mónica Formation*	
MID- to PALEO-PROTEROZOIC	Buenos Aires Complex					

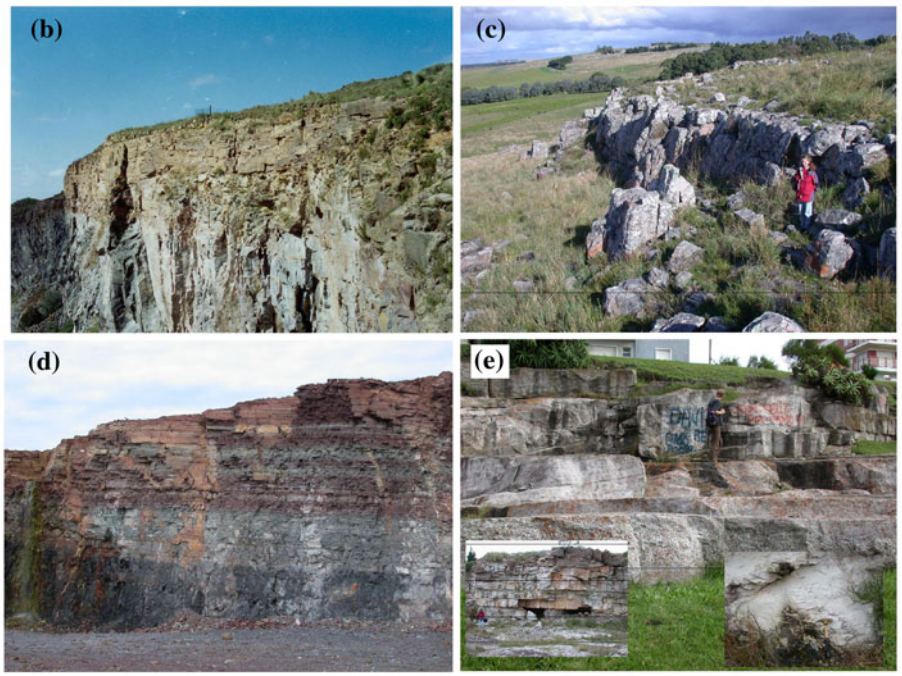

Fig. 2 **a** Stratigraphic table of the Tandilia System (based on Poiré et al. 2003; revised after Zimmermann and Spalletti 2009). **b** Contact between the metaigneous basement and the Villa Mónica Formation. **c** Exposure of the quartz-arenites of the Cerro Largo Formation. **d** Fine-grained clastic sedimentary rocks of the Cerro Negro Formation. **e** Quartz-arenites of the Balcarce Formation with tuff beds (*inlet lower left*) and the Hirnantian glacial diamictite (*lower right inlet*)

The Cerro Negro Formation (La Providencia depositional sequence; Fig. 2a and d) exceeds 150 m in thickness and is characterised by mudstones and marls, fine-grained sandstone-mudstone intercalations, mainly formed in upper to lower tidal-flats and epiclastic rocks as well as pyroclastites. Acritarchs were reported by Cingolani et al. (1991), consisting of simple forms like sphaeromorphis such as *Synsphaeridium* sp., *Trachysphaeridium* sp. and *Leiosphaeridia* sp., and are reinterpreted by Gaucher and Poiré (2009a). They determine an Uppermost Ediacaran age for the microfossil assemblages.

Age constraints for the entire succession are not perfectly established so far. Early Rb–Sr analyses on whole rock samples gave ages between 800 and 650 Ma for all formations (Cingolani and Bonhomme 1982; Kawashita et al. 1999), which cannot be substantiated by palaeontological finds. However, stromatolite occurrence in the Villa Mónica Formation shows structures typical for

Cryogenian-Tonian deposits (Poiré 1989). Acritarch populations in the Cerro Largo and Cerro Negro Formations point to a Late Ediacaran age and coincide with C-isotope curves (Fig. 2). *Cloudina* sp. was found in the Loma Negra Formation (Gaucher et al. 2005), which would reduce the age range of this formation to, not older than 555.2 ± 6.1 Ma, as the oldest well-dated *Cloudina* sp. occurrence found in the Dengying Formation below the well-dated Doushantuo-Dengying boundary indicates (Zhang et al. 2005). This is supported by the recent secular curve for C isotopes by Halverson et al. (2010), where the primary values for the Loma Negra Formation (Gómez Peral et al. 2007) would fit in the latest Ediacaran, and is confirmed by the occurrence of recently defined late Ediacaran Leiosphere Palynoflora for southwest Gondwana (Gaucher and Sprechmann 2009), bracketed between 565 Ma (Grey and Calvert 2007) and 542 Ma (Gaucher and Sprechmann 2009) in the Cerro Negro Formation. The Cerro Negro Formation contains typical acritarchs of this fauna but no Cambrian micro- or macrofossils (Gaucher and Poiré 2009a). The contact between the Loma Negra Formation and the Cerro Negro Formation is marked by a karst surface (see above). This karst surface is interpreted as related to a regional event and was correlated with occurrences in western South Africa (Nama Group) and southern Paraguay (Gaucher and Poiré 2009b). In both correlation horizons, the rocks were dated at c. 545 Ma with radiometric techniques (U–Pb on volcanic zircons from tuff beds). This all would propose a depositional age between 545 and 542 Ma. Recent palaeomagnetic studies (Rapalini et al. 2008) propose a slightly younger age for the formation, which is based on the assumption that the Rio de la Plata craton already merged with Gondwana at 550 Ma, which is controversial for this specific region (Gaucher et al. 2008).

Earlier, glacial deposits were proposed as being part of the stratigraphy (Iñiguez Rodríguez 1999; Pazos et al. 2008; Gaucher et al. 2008) without any age constraint (Poiré 2004; Van Staden et al. 2010). For the Sierra de Volcán diamictite (Fig. 2), an Ordovician age was established (Van Staden et al. 2010) and interpreted as a facies variation of the Balcarce Formation (Zimmermann and Spalletti 2009). Detrital zircon age dating of the Sierras Bayas Group was unsuccessful in obtaining a reliable sedimentation age, as the youngest detrital zircon is not younger than Mesoproterozoic (Gaucher et al. 2008).

The major unconformities between the different successions (in grey in Fig. 2) can be interpreted as basin wide and is reflected in the change of the mineralogical composition of the different successions (Poiré 1987). The contact between the Villa Mónica and the Cerro Largo Formations is marked by an unconformity (Fig. 2a) with a brecciated deposit. The diagenetic grade is higher below this unconformity then above. Diagenetic microfabrics in rocks of the Villa Mónica Formation show characteristics related to late or deep mesodiagenesis pointing to more than 3 km of burial depth (Gómez Peral 2008). In contrast, the Cerro Largo and Loma Negra Formations microfabrics are typical for early to middle mesodiagenesis (Gómez Peral 2008). Hence, we consider the unconformity between Villa Mónica and Cerro Largo Formations as representing a large period of erosion (at least 1,000 m of sediments and 200 Ma; Gómez Peral 2008) to effectuate the lower diagenesis grade of the Cerro Largo Formation. Therefore, it shows that the Sierras Bayas Group and the Cerro Negro Formation reflect the geological evolution bracketed between c. 850 and 490 Ma, while the upper limit is determined by the occurrence of Neoproterozoic stromatolite types in the Sierras Bayas Group (Gómez Peral et al. 2007), and the lower limit drawn by the occurrence of Ordovician trace fossils in the overlying Balcarce Formation (Seilacher et al. 2003).

Palaeocurrents were measured for the Villa Mónica, Cerro Largo and Cerro Negro Formations. Those in the Villa Mónica Formation ($n = 26$) are measured in asymmetrical stromatolitic domes and point for a stromatolitic platform in a shallow marine system to a main sediment source in the west (Poiré 1987). In the Cerro Largo Formation ($n = 71$), ripples and cross-bedding sedimentary structures were used as palaeocurrent indicator and point to sources in the north and an open marine environment in the south (Poiré 1987). However, data from the Cerro Negro Formation are sparse ($n = 4$) and measured in sub-aqueous ripples and infer sources in the west and north, with the coastline interpreted to be east–west orientated (Andreis et al. 1992).

Regional geological background

The unfolded and not metamorphosed supracrustal rocks in the Tandilia System were not penetrated by magmatic events, except one possible dyke event in the Sierras Barrientos (Celesia et al. 2008). Such an exceptional geological setting is not known in southwest Gondwana during the Ediacaran, besides in the Nama Group (Fig. 1a; Tankard et al. 1982; Basei et al. 2000). During the Early Neoproterozoic, the supercontinent Rodinia broke up and possibly several oceanic basins developed between the Congo, Kalahari and Río de la Plata cratons and probably some minor fragments (e.g. Gray et al. 2006). Throughout the Ediacaran and/or the Lower Palaeozoic, these basins were closed involving large volcanic arcs and associated subduction zones with terrane/craton reorganisation between 550 and 480 Ma (Frimmel et al. 1996; Frimmel and Fölling 2004; Gray et al. 2006; Gresse et al. 2006; Rapela et al. 2007; Gaucher et al. 2008; Oyhantçabal et al. 2009; Drobe et al. 2010). However, oceanic crust fragments, associated arc basins or arc-related detritus have not

been identified beyond doubt, so far. Earlier, mafic rocks exposed along the modern western margin of the Kalahari Craton were interpreted as the suture between the Kalahari and Río de la Plata craton (Frimmel et al. 1996), but are now explained to be retro-arc basin magmas (Basei et al. 2008). Palaeotectonic models changed and varied regarding the orientation of the subduction and the exact location of the oceanic basins, as subduction was interpreted as being directed to the west (e.g. Frimmel et al. 1996) or east (e.g. Basei et al. 2000, 2008). Reconnaissance studies suspect possible arc-related detritus by geochemical means (Basei et al. 2005), but the age and provenance is unfortunately unknown. Hence, the deposition of the Sierras Bayas Group and the Cerro Negro Formation was somewhat shielded from these regional tectonic processes. However, further south of the Tandil range, Gregori et al. (2004) reported intrusive bodies in the Sierra de Ventana belt (Fig. 1a), related to an arc and post-collisional events, which implicates an active continental margin with a probable subduction zone environment during the Ediacaran and Early Cambrian, probably surrounding parts of Gondwana as proposed by Cawood (2005), and reported by Chew et al. (2008) from western South America. Today, the southern boundary of the Río de la Plata craton is adjoined to Patagonia, but the position of the latter during the Neoproterozoic is not known (Rapela et al. 2003; Pankhurst et al. 2006). Rapela et al. (2007) and Gaucher et al. (2008) used detrital zircon ages to understand the geological evolution of the Río de la Plata Craton. Their results point to a subordinated influence of Archaean sources, but major peaks in the age distribution are represented by Early Palaeoproterozoic, Mesoproterozoic (1.5 and 1.0 Ga) and Neoproterozoic to Lower Palaeozoic detritus. Major deposition of Mesoproterozoic and Neoproterozoic detritus could only be found in Lower Palaeozoic quartz-arenites (Rapela et al. 2007) and glacial diamictites (Van Staden et al. 2010). No tectonic influence of the Neoproterozoic rift-drift and collision-related tectonic events are visible in the Tandilia region. This is in contrast to studies of the Neoproterozoic to Lower Palaeozoic Arroyo del Soldado Group in Uruguay, where nearly 1-km-thick massive conglomeratic successions (Barriga Negra Formation; Blanco et al. 2009), which is absent in the Sierras Bayas Group, revealed a dominant input of Ediacaran detrital zircons (Blanco et al. 2009).

Sampling and methodology

Sampling

The large number of rock samples was collected only in well-studied lithostratigraphic sections. Representative samples were selected for geochemistry according to their position in the lithostratigraphy to cover as many different lithotypes as possible.

Petrography and mineralogy

Polished thin section samples were used for petrographic analyses in a polarising microscope (Olympus B60XM; UiS). Hand-crushed and hand-grinded rock samples were used for X-ray powder diffraction. X-ray diffraction (XRD) analyses were carried out on fine meshed sample material (2–5 μm) (Moore and Reynolds 1989), measured with a Philips PW 1011/00 diffractometer, with Cu lamp ($k\alpha = 1.5403$ Å) operated at 18 mÅ and 36 kV at the Centro de Investigaciones Geológicas (La Plata, Argentina). The samples were measured from 2 to 40° 2θ, in steps of 0.02°/2 s.

The identification and characterisation (shape, size, fractures, inclusions, etc.) of heavy minerals and matrix of the clastic rocks were done using a scanning and backscattered electron microscope using a Zeiss Supra 35 VP scanning and backscattered electron microscope equipped with EDAX EDS. The system was set at 15 keV, a working distance of 20 mm and a live time of 60 s per spot; Genesis software was used for data acquisition/reduction (SEM-BSE-EDS; UiS).

Geochemistry

Powders were prepared by milling to a very fine mesh. Pressed powder pellets (for selected trace elements) contain 8.0 g of sample powder mixed with 4 g of binder, placed in an aluminium cup and pressed at a pressure of 20 tons. Glass beads (for major elements) were prepared by fusing sample powder with a flux containing 50% lithium metaborate and 50% lithium tetraborate with $LiNO_3$ as oxidant. XRF precision and accuracy were controlled by international and internal rock standard and below 5% (1 s) for measured elements. Neutron activation analyses (INAA) were performed by ACTLABS (Ontario, Canada) to obtain trace elements (rare earth elements, Th, Sc, Ta, Hf, Cs, Co, As, base metals (not reported here), Mo, U). Sample powders were dissolved in lithium metaborate flux and the resultant bead promptly digested in dilute nitric acid. INAA precision and accuracy based on replicate analysis of international rock standards are 2–5% (1σ) for most elements and ±10% for U, Sr, Nd and Ni (Ni and Sr were measured with XRF).

Petrography

Petrographic and XRD data are only briefly discussed here as previous studies presented the results in detail (Poiré 1987; Gómez Peral et al. 2007). The oldest deposit, the Villa Mónica

Formation, is characterised by poorly sorted and immature rocks at its base and composed of undulose quartz, polycrystalline quartz, alkali-feldspar and lithoclasts of mainly metasedimentary origin. The clay-rich matrix (20%) comprises mainly illite, quartz and albite. At the top of the formation, the grains are rounded, better sorted (80–120 μm) and the often only components are alkalifeldspar and quartz. These quartz-arenites are associated with very fine-grained, partly dedolomitised, marls composed of dolomite, calcite, illite (rarely layered illite–smectite), quartz and albite. The rocks of the Cerro Largo Formation display poorly sorted but mineralogically mature deposits, where quartz (mostly undulose and rarely polycrystalline) is the most abundant mineral embedded in a secondary quartz cement. All other minerals, like alkalifeldspar (microcline could be identified often), mica, kaolinite, goethite, chlorite and zircon, are very rare. The only lithoclasts found, derived from metasedimentary rocks. The samples of the Olavarría Formation consist mainly of fine-clastic rocks intercalated with sandstones. The siltstones comprise quartz, muscovite, calcite, microcline, biotite, illite, chlorite and haematite. The stratigraphically equivalent quartz-rich sandstones of the Las Águilas Formation are compositionally similar, but slightly coarser grained and display additional rutile, glauconite and haematite. The Cerro Negro Formation comprises different lithotypes (sandstones, marls, siltstones and mudrocks) and reflects in some cases a strong input of carbonate material, most probably derived from the underlying carbonates. The clastic rocks are mostly texturally and mineralogically immature silty wackes, rich in quartz, mica (mainly biotite) and partly plagioclase. Some samples display carbonate and sedimentary lithoclasts (siltstones and silty wackes), dark-brown wavy fragmented clayey lithoclasts and small amphiboles, but rarely metamorphic lithoclasts and polycrystalline quartz. The matrix comprises, besides quartz, mica, haematite, chlorite-montmorillionite, titano-magnetite, illite, rutile, calcite and titanite. Some beds show reworking of muddy and clayey (chlorite, illite) material and the occurrence of flame-like, elongated fragments, shard-like clasts, and point to a volcanic origin. Such altered pyroclastic deposits of the Sierras Bayas Group and Cerro Negro Formation were identified and described by Dristas and Frisicale (1984), Frisicale and Dristas (2000) and Poiré et al. (2003).

Geochemistry

Major element geochemistry and alteration

Major element geochemistry

Most of the rocks from the Villa Mónica Formation are enriched in silica and depleted in nearly all other major elements. Exceptions are some rocks of the outcrop El Polvorín (Fig. 1b), where the samples are enriched in Al_2O_3 and represent kaolinite-rich shales and those from Tres Antenas, which are represent carbonate-rich shales (Table 1 data repository). Samples at the base of the formation are slightly depleted in silica and therefore show higher concentrations in other major elements. The samples of the Cerro Largo Formation are enriched in silica (<98%) and therefore, depleted in other major element. Only few samples have lower silica concentrations (<80%) and are enriched in Al_2O_3, K_2O or iron. The samples from the Las Águilas Formation are comparable to the less silica-rich samples of the former formation. In contrast, samples of the Olavarría Formation are less enriched in silica than those of the Las Águilas Formation and display therefore higher concentrations in all other major elements and with few samples enriched in CaO. Most of the samples of the Cerro Negro Formation have major element concentrations comparable with typical upper continental crust (Table 1 data repository; UCC, after McLennan et al. 2006). Some samples are enriched in CaO (reflecting calcite), Al_2O_3 and MgO (reflecting clay minerals) or iron. However, K_2O enrichments can be observed but rarely those in Na_2O. Marls are enriched in CaO and rarely MgO and support the existence of calcite as major carbonate mineral.

Alteration

The use of major element geochemistry, in particular, should be treated with caution due to their possible mobility and redistribution during chemical weathering and diagenesis (e.g. Nesbitt 2003). However, it can be applied to determine the degree of alteration (Nesbitt and Young 1982; Fedo et al. 1995; von Eynatten et al. 2003). The Chemical Index of Alteration (CIA; Nesbitt and Young 1982) and K/Cs ratios (McLennan et al. 1993) are two possible measures for quantification. Figure 3a shows the relations of Al–Ca + Na–K as molar units to determine alteration trends; samples with high silica and Ca values are excluded. This accounts also for the abundant marls (Table 1 data supplementary). The CaO content in these rocks does not reflect the alteration of the clastic component and can therefore not used to determine the CIA in the sense of Nesbitt and Young (1982). The samples of the Villa Mónica Formation shows CIA values between 71 and 90, with the latter value due to high amount of Al_2O_3 as a result of kaolinisation in these specific samples. A trend for this formation cannot be observed. Samples of the Cerro Largo Formation are slightly higher and comparable in their CIA values with the one of the Las Águilas Formation with values above 70. Rocks of the Olavarría Formation are comparable in their spread with the samples of the Cerro

Table 1 Selected major and trace element abundances and ratios for rocks of the Sierras Bayas Group and the Cerro Negro Formation (*bdl* below detection limit, *sye* syenite, *mon* monzonite, *c-are* coarse arenite, *wa* wacke, *are* arenite, *con* conglomerate, *sh* shale, *qa* quartzarenite, *si* siltstone, *BM* basement rocks (Buenos Aires Complex, *VMF* Villa Mónica Formation, *CLF* Cerro Largo Formation, *LAF* Las Águilas Formation, *OLF* Olavarría Formation, *CNF* Cerro Negro Formation). Unreliable CIA, Cr, Ta and Co values are deleted, please see Table 1 data repository for all values

Sample	Rock type	CIA	SiO_2 wt%	$A1_2O_3$ wt%	MgO wt%	CaO wt%	K_2O wt%	TiO_2 wt%	Cs ppm	Nb ppm	Ta ppm	Y ppm	Zr ppm	Hf ppm	Sc ppm	Th ppm
BM 02-343	sye	75	75.9	16.34	0.40	0.61	2.69	0.16	1.2	3.9	0.3	17.1	88	2.9	2	4.8
BM 02-347	mon		51.3	15.82	5.49	7.75	1.26	0.84	0.4	7.5	0.4	18.4	107	2.7	37	0.3
BM 02-344	sye		62.4	17.99	0.52	1.72	7.81	0.45		3.8		7.1	163			9.8
BM 02-34S	sye	53	73.2	14.13	0.31	0.99	5.27	0.11		2.6		09	192			10.6
VMF 02-349	c-are		80.9	12.10	0.51	0.20	3.94	0.19	1	5.8	0.5	1.5	129	3	1.7	1.6
VMF 02-350	c-are		85.6	6.88	0.15	0.09	3.22	0.17	0.5	3.3	0.3	1.5	98	3	1.5	1.7
VMF 02-351	c-are		86.1	7.44	0.19	0.12	3.66	0.14	7	3.3	0.3	1.5	91	2	1.6	2
VMF IN-1	sh		46.3	29.38	2.61	1.67	9.05	1.60	12	46.7	2.8	14.5	456	12	14.4	23.8
VMF IN-2	sh	71	47.1	31.23	1.90	0.76	9.89	1.66	10	46.8	2.3	11.2	509	13	15.3	23.2
VMF IN-3	sh	71	48.7	29.71	2.24	1.14	9.15	1.38	14	38.7	2.2	14.8	368	10	14.5	20.1
VMF 02-299	qa		96.3	0.24	0.11	0.03	0.31	0.07	1	7	0.5	1.5	57	2	1.5	3
VMF 02-300	qa		92.1	4.17	0.15	0.08	0.32	0.09	0.9	10.1	0.6	1.5	56	1	0.9	2
VMF 02-301	qa		94.9	0.09	0.11	0.03	0.26	0.06	1	5.7	0.5	1.5	43	1	1.3	2
VMF 02-302	qa		95.8	0.10	0.10	0.03	0.23	0.06	0.5	7.5	0.5	1.5	34	1	1.1	3
VMF 02-304	qa		89.6	4.64	0.21	0.08	0.50	0.08	0.9	8.5	0.5	1.5	48	1	1.7	3
VMF T6EP 35,5	sh	90	66.9	24.46	0.10	0.01	1.63	1.58	1	56	4.1	160.1	708	20	11	17
VMF T6EP 42,7	qa		86.6	9.69	0.05	0.02	1.65	0.11	1	5.5	0.4	1.4	121	3	1	1.6
VMF T6EP 50,5	sh		62.7	22.73	0.54	0.22	6.02	0.65	3	14.8	0.5	4.1	445	13	6.1	7.8
VMF T6EP 53,1	sh	74	63.6	20.22	0.66	0.22	5.56	0.64	4	17.6	0.6	2.8	653	20	7.9	12
VMF PELV-VM	sh	72	70.3	18.69	1.24	0.25	5.38	0.87		28.8	0.1	7.2	427			12.2
CLF 02-305	qa		95.6	3.02	0.06	0.01	0.12	0.03	1	1.1	0.1	1	31	1	0.3	0.5
CLF 02-306	qa		96.2	1.05	0.03	0.04	0.07	0.02	0.8	2.9	0.2	2	32	1	0.4	0.5
CLF 02-307	qa		97.9	0.74	0.05	0.03	0.05	0.02	1	0.9	0.1	1.5	34	1	0.2	0.3
CLF 02-308	qa		97.0	0.62	0.09	0.02	0.05	0.02	0.9	1.1	0.1	1.5	31	1	0.2	0.4
CLF 02-310	qa		97.2	1.73	0.02	0.04	0.02	0.02	0.9	2.9	0.3	2.5	33	1	0.2	0.3
CLF 02-335	qa		95.7	3.89	0.02	0.05	0.02	0.01	56.9	16.3	0.5	34.2	173	8	0.1	bdl
CLF 02-336	qa		93.1	4.31	0.02	0.05	0.04	0.02	0.9	2.8	0.2	2.8	21	4	0.1	bdl
CLF 02-337	qa		93.6	4.62	0.05	0.05	0.04	0.01	0.8	7	0.5	21.9	170	5	bdl	2.1
CLF 81002-A	are		81.6	9.91	0.48	0.17	1.87	0.39	1	19.5	1.3	44.5	444	11	10.5	16
CLF 81002-H	are		73.9	3.92	0.18	0.20	0.10	0.03	1	4.3		12	25	2	3.8	1.6
CLF CL1	sh		89.3	7.06	0.22	0.04	1.11	0.12	1	6		4.8	68	4	2.3	2.4
CLF GL02	qa		91.6	1.77	0.13	0.05	0.74	0.07	0.8	3.2	0.3	2.5	52	2	1.7	2.1
CLF GL03	qa		92.4	2.12	0.12	0.05	0.80	0.10	1	3.5	0.3	4.3	65	2	1.8	2.6

Table 1 continued

Sample	Rock type	CIA	SiO_2 wt%	$A1_2O_3$ wt%	MgO wt%	CaO wt%	K_2O wt%	TiO_2 wt%	Cs ppm	Nb ppm	Ta ppm	Y ppm	Zr ppm	Hf ppm	Sc ppm	Th ppm
CLF 02-339	qa		97.1	1.28	0.04	0.01	0.02	0.03		2.8		2.5	31			2.5
CLF 02-340	qa		95.7	2.34	0.05	0.00	0.02	0.04		2.3		1.5	20			3.5
CLF 81002-17	qa		98.2	1.02	0.03	0.05	0.07	0.05		2.3		5	52			1.9
CLF 81002-2	qa	74	78.1	8.51	0.65	0.09	1.93	0.17		5		13.4	123			9.7
CLF 81002F	are		81.9	11.50	0.22	0.18	1.41	0.11		3.8		2.5	56			3
CLF 81002A1	are	82	73.9	16.91	0.75	0.20	2.37	0.39		8.1		12.1	249			7.7
CLF 81002-D	are	73	76.9	4.82	0.33	0.09	0.84	0.10		4.2		2.5	78			2
CLF 81002-G	qa		94.1	4.46	0.09	0.04	0.23	0.06		6.6		4.5	31			1.4
CLF CL2A	qa		93.0	3.79	0.08	0.13	0.64	0.10		3		2.5	26			1.3
CLF CL2	qa		95.0	1.60	0.07	0.12	0.61	0.10		6.7		4.5	27			1.5
CLF GL01	qa		92.4	3.97	0.23	0.11	0.89	0.08		3.1		5.2	48			3.1
CLF GL01A	qa		91.2	3.85	0.24	0.10	0.86	0.08		2.8		4.9	48			3.3
CLF ARGLAUC	are	72	77.1	11.10	0.95	0.16	2.91	0.22		6.3		17.3	126			10.3
LAF CAR 8	are		86.7	7.56	0.25	0.04	2.98	0.04	1	3 2.8	0.3	2.9	28	1	0.7	1.2
LAF CAR 2-10	sh		88.7	6.02	0.17	0.02	1.29	0.12	1	5.2	0.4	7	107	3	3.2	4.9
LAF CAR 2-8,5	are		87.0	6.42	0.13	0.05	1.60	0.10	1	3.8	0.3	4.4	99	3	4.2	4
LAF CAR 2-7	are	75	77.4	15.6097	0.22	0.11	3.33	0.64	2	16.3	1.6	24	471	13	14.4	15
OLF PEL INTRA C	sh		56.8	16.97	1.28	5.24	4.54	0.63	18	11.1	0.6	90.6	95	6	18.1	11
OLF 02-331	sh	72	80.3	7.96	0.34	0.16	2.48	0.70	3	11.5	1.2	34.6	727	23	6.9	12
OLF 02-333	sh	69	68.8	15.37	1.08	0.25	5.27	1.07	7	18.7	1.9	31.2	243	7	13	14
OLF 02-332	sh	75	71.4	12.14	0.52	0.25	2.48	0.54		10.7		33.3	302			
OLF 02-334	sh	70	69.5	16.03	1.08	0.23	5.09	0.93		16.4		32	172			
OLF 02-334A	sh	69	69.8	15.19	1.10	0.22	5.11	0.93		16.4		32.1	171			
OLF PSAMPELCL	sh	77	74.8	15.56	0.58	0.31	2.89	0.51		9.3		13.7	296			10.9
OLF CLlb	sh	65	71.1	14.58	1.22	1.01	4.69	0.84		15.7		26.6	309			14.4
OLF PELGCL	sh		66.8	12.98	1.30	3.47	3.65	0.67		12.6		27.8	188			9
OLF CL3	sh	67	57.3	11.80	0.95	7.85	4.35	0.65		16.9		21.2	217		12.3	14.5
CNF 02-322	sh		68.5	15.28	1.44	1.04	3.70	0.75	9	14.5	0.8	28.1	233	8	12.3	11
CNF 02-324	sh		60.7	15.85	1.87	6.12	4.14	0.81	8	15.5	1	37.1	184	6	12.9	8.8
CNF 02-326B	sh	72	62.9	19.35	1.37	0.30	5.35	1.05	14	20.3	1.2	8.2	252	8	17.5	12
CNF 02-326C	are		84.0	4.14	0.16	5.09	0.36	0.08	0.9	4		18.3	27	2	3.2	0.9
CNF 02-326D	are		76.7	4.23	0.16	9.15	0.40	0.23		3		20.6	35			1.4
CNF CN 66,45	are	74	56.1	19.47	2.42	0.51	4.57	0.75	17	16.7		34.7	129	4	15.8	10
CNF CN60,2	are	69	57.9	18.77	2.32	1.06	4.68	0.81	22	15.7	1.1	43.9	115	3	14	8.1
CNF CN 66,15	are	71	51.9	19.37	2.34	0.47	5.47	0.93	17	18.8		53	139	4	21.8	17

Table 1 continued

Sample	Rock type	CIA	SiO_2 wt%	$A1_2O_3$ wt%	MgO wt%	CaO wt%	K_2O wt%	TiO_2 wt%	Cs ppm	Nb ppm	Ta ppm	Y ppm	Zr ppm	Hf ppm	Sc ppm	Th ppm
CNF CNCH	qa		82.7	9.27	0.53	0.23	1.89	0.26	4	6.3	0.8	1.5	66	2	5.6	2.5
CNF 180602-21	si		70.5	11.48	1.66	1.79	1.69	0.67	5	13.2		34.2	198	7	10	10
CNF 180602-29	si	73	56.4	19.56	2.68	0.42	4.36	0.89	12	17.5		47.3	190	6	18.8	16
CNF 180602-48	si	75	55.5	21.52	2.61	0.40	4.20	0.88	12	17.2		38.3	162	5	19.8	16
CNF 190602-06	si	73	66.0	16.25	2.36	0.36	2.36	0.61	5	13.2		31.2	196	6	10.3	10
CNF 190602-18	si	72	63.1	16.86	2.72	0.39	3.23	0.74	9	15.6		162.7	173	6	13.7	11
CNF 190602-53	si	61	65.0	15.11	2.33	0.65	3.08	0.80	9	16.3		34.6	125	4	14.3	7.9
CNF 190602-57	si	69	66.3	14.63	2.25	0.46	2.18	0.74	8	14.7		32.8	204	6	10	10
CNF 190602-32	si	89	64.4	16.99	2.56	0.47	0.40	0.23	7	11.5		28.9	196	6	10.7	11
CNF 02-322-A	sh	72	72.7	16.49	1.04	0.97	3.29	0.75		14.7		26.8	232			
CNF 02-326DP	sh		70.5	5.31	0.10	12.78	0.08	0.02		1.8		2.1	10			1.1
CNF CN63,5	sh	70	58.7	19.09	2.60	0.45	5.80	1.09		20.5		40.3	184			20.2
CNF 180602-04	sh	72	51.1	22.18	3.15	0.46	5.62	1.00		19		37	158			17.6
CNF 180602-40	sh	62	69.1	11.25	1.94	0.52	1.51	0.45		11.8		21.2	123			7.9
CNF 180602-58	sh		49.8	12.90	2.13	11.79	1.98	0.67		14		87.5	139			9
CNF 190602-02	sh	76	61.6	15.85	2.82	0.33	1.72	0.60		12.7		36.7	138			8.1
CNF 190602-14	sh	70	67.4	14.35	2.37	0.27	2.26	0.67		13.9		27.9	161			8.6
CNF 190602-39	sh	65	58.5	14.60	3.20	0.39	2.58	0.50		14.7		35.4	136			10.1
CNF 190602-45	sh		63.9	12.31	2.25	4.65	1.41	0.81		15.8		58	313			14.1

Sample	Rock type	U ppm	La ppm	LaN/YbN	Eu/Eu*	Ce/Ce*	Th/Sc	Zr/Sc	Ti/Zr	La/Sc	Nb/Y	Zr/Ti	K/Cs
BM 02-343	sye	1	20	8.69	0.67	0.88			10.86		0.23	0.09	
BM 02-347	mon	0.2	21	7.40	1.06	1.02			47.24		0.41	0.02	
BM 02-344	sye								16.50		0.54	0.06	
BM 02-34S	sye								3.47		2.89	0.29	
VMF 02-349	c-are	0.4	10	16.89	0.70	0.96	0.94	76.00	8.82	5.88	3.87	0.11	32706
VMF 02-350	c-are	0.3	10	22.52	*0.89*	0.94	1.13	65.07	10.56	6.67	2.20	0.09	53442
VMF 02-351	c-are	0.4	13	29.28	0.63	1.01	1.25	57.13	9.18	8.13	2.20	0.11	4340
VMF IN-1	sh	1.8	85	17.84	0.43	0.89	1.65	31.64	21.07	5.87	3.22	0.05	6258
VMF IN-2	sh	2.3	82	16.38	0.52	0.90	1.52	33.24	19.57	5.39	4.18	0.05	8206
VMF IN-3	sh	2.2	65	15.78	0.52	0.91	1.39	25.40	22.41	4.51	2.61	0.04	5425
VMF 02-299	qa	0.15	8	14.19	0.47	0.98	2.00	37.87	7.60	5.60	4.67	0.13	2565
VMF 02-300	qa	0.2	13	21.96	0.63	1.01	2.22	62.22	9.63	14.44	6.73	0.10	2961
VMF 02-301	qa	0.15	8	28.38	0.66	1.03	1.54	33.15	8.21	6.46	3.80	0.12	2150
VMF 02-302	qa	0.1	10	33.79	0.57	1.09	2.73	30.45	10.92	9.09	5.00	0.09	3802

Table 1 continued

Sample	Rock type	U ppm	La ppm	LaN/YbN	Eu/Eu*	Ce/Ce*	Th/Sc	Zr/Sc	Ti/Zr	La/Sc	Nb/Y	Zr/Ti	K/Cs
VMF 02-304	qa	0.15	9	19.60	0.75	0.93	1.76	28.24	9.49	5.12	5.67	0.11	4630
VMF T6EP 35,5	sh	1.4	159	9.77	0.60	1.16	1.55	64.40	13.40	14.45	0.35	0.07	13489
VMF T6EP 42,7	qa	0.2	17	19.15	*0.99*	1.09	1.60	120.60	5.47	17.00	3.93	0.18	13697
VMF T6EP 50,5	sh	0.6	47	24.43	0.95	1.03	1.28	72.93	8.72	7.70	3.61	0.11	16663
VMF T6EP 53,1	sh	0.7	61	24.09	0.86	0.97	1.52	82.65	5.89	7.67	6.29	0.17	11536
VMF PELV-VM	sh								12.14		4.000	0.08	
CLF 02-305	qa	0.1	5	11.71	*0.92*	0.83	1.67	104.67	4.77	17.33	1.10	0.21	996
CLF 02-306	qa	0.1	5	10.81	*0.92*	0.79	1.25	79.75	4.13	12.00	1.45	0.24	674
CLF 02-307	qa	0.05	5	10.36	*1.00*	0.82	1.50	170.00	3.35	23.00	0.60	0.30	415
CLF 02-308	qa	0.1	4	8.56	*1.09*	0.69	2.00	154.00	3.11	19.00	0.73	0.32	461
CLF 02-310	qa	0.05	5	12.16	*1.00*	0.54	1.50	167.00	3.23	27.00	1.16	0.31	194
CLF 02-335	qa	0.05	3	6.98	*1.20*	0.50		1725.00	0.35	31.00	0.48	2.88	3
CLF 02-336	qa	0.05	2	3.38	*1.34*	1.15		212.00	5.37	15.00	1.00	0.19	387
CLF 02-337	qa	0.5	2	3.38	*1.34*	1.15			0.39		0.32	2.58	405
CLF 81002-A	are	2.3	68	11.47	0.65	1.20	1.52	42.30	5.32	6.47	0.44	0.19	15515
CLF 81002-H	are	1	10	5.63	0.64	0.80	0.42	6.45	6.85	2.63	0.36	0.15	830
CLF CL1	sh	0.5	26	21.96	0.48	1.28	1.04	29.70	10.36	11.30	1.25	0.10	9198
CLF GL02	qa	0.5	14	18.92	0.46	1.17	1.24	30.53	8.20	8.24	1.28	0.12	7678
CLF GL03	qa	0.5	27	26.06	0.43	1.29	1.44	36.33	8.98	15.00	0.81	0.11	6599
CLF 02-339	qa								6.32		1.12	0.16	
CLF 02-340	qa								11.15		1.53	0.09	
CLF 81002-17	qa								5.30		0.46	0.19	
CLF 81002-2	qa								8.49		0.37	0.12	
CLF 81002F	are								11.29		1.52	0.09	
CLF 81002A1	are								9.44		0.67	0.11	
CLF 81002-D	are								7.70		1.68	0.13	
CLF 81002-G	qa								10.81		1.47	0.09	
CLF CL2A	qa								23.06		1.20	0.04	
CLF CL2	qa								22.26		1.49	0.04	
CLF GL01	qa								10.01		0.60	0.10	
CLF GL01A	qa								9.89		0.57	0.10	
CLF ARGLAUC	are								10.51		0.36	0.10	24737
LAF CAR 8	are	0.3	10	16.89	0.33	1.39	1.71	39.29	8.94	14.29	0.97	0.11	24737
LAF CAR 2-10	sh	0.5	18	12.16	0.49	1.32	1.53	33.44	6.84	5.63	0.74	0.15	10708
LAF CAR 2-8,5	are	0.6	14	11.83	0.55	1.33	0.95	23.60	5.93	3.33	0.86	0.17	13265

Table 1 continued

Sample	Rock type	U ppm	La ppm	LaN/YbN	Eu/Eu*	Ce/Ce*	Th/Sc	Zr/Sc	Ti/Zr	La/Sc	Nb/Y	Zr/Ti	K/Cs
LAF CAR 2-7	are	5.6	49	8.95	0.64	1.22	1.04	32.69	8.20	3.40	0.68	0.12	13817
OLF PEL INTRA C	sh	2.3	4	4.03	0.62	0.98	0.61	5.27	39.59	3.00	0.12	0.03	2094
OLF 02-331	sh	3.6	26	3.59	0.52	1.15	1.74	105.36	5.78	3.77	0.33	0.17	6848
OLF 02-333	sh	3.6	48	9.54	0.53	0.97	1.08	18.67	26.31	3.69	0.60	0.04	6245
OLF 02-332	sh								10.75		0.32	0.09	
OLF 02-334	sh								32.46		0.51	0.03	
OLF 02-334A	sh								32.62		0.51	0.03	
OLF PSAMPELCL	sh								10.26		0.68	0.10	
OLF CLlb	sh								16.28		0.59	0.06	
OLF PELGCL	sh								21.46		0.45	0.05	
OLF CL3	sh								18.00		0.79	0.06	
CNF 02-322	sh	2.6	27	5.53	0.58	1.02	0.89	18.98	19.34	2.20	0.52	0.05	3414
CNF 02-324	sh	1.8	30	6.14	0.57	1.02	0.68	14.24	26.47	2.33	0.42	0.04	4296
CNF 02-326B	sh	4.6	11	3.10	0.57	0.60	0.69	14.37	24.96	0.63	2.48	0.04	3172
CNF 02-326C	are	2.2	16	8.32	0.50	0.80	0.28	8.53	18.01	5.00	0.22	0.06	3320
CNF 02-326D	are		2						38.21		0.15	0.03	
CNF CN 66,45	are	1.8	38	7.78	0.63	0.99	0.63	8.16	34.85	2.41	0.48	0.03	2232
CNF CN60,2	are	1.4	32	6.36	0.56	1.02	0.58	8.18	42.41	2.29	0.36	0.02	1766
CNF CN 66,15	are	3.2	69	9.70	0.45	0.96	0.78	6.39	39.81	3.16	0.35	0.03	2671
CNF CNCH	qa	0.7	4	3.86	0.73	0.49	0.45	11.71	23.94	0.71	4.20	0.04	3922
CNF 180602-21	si	1.8	27	5.21	0.48	1.05	1.00	19.75	20.43	2.70	0.39	0.05	2799
CNF 180602-29	si	2.2	58	8.66	0.54	0.97	0.85	10.09	28.05	3.07	0.37	0.04	3015
CNF 180602-48	si	2.7	50	8.66	0.59	0.97	0.81	8.20	32.65	2.53	0.45	0.03	2903
CNF 190602-06	si	2.4	32	6.36	0.49	0.99	0.97	19.03	18.66	3.11	0.42	0.05	3918
CNF 190602-18	si	1.9	42	7.88	0.46	1.01	0.80	12.60	25.70	3.07	0.10	0.04	2979
CNF 190602-53	si	2.3	34	7.66	0.47	0.97	0.55	8.72	38.65	2.38	0.47	0.03	2844
CNF 190602-57	si	2.4	29	5.94	0.65	1.07	1.00	20.40	21.83	2.90	0.45	0.05	2260
CNF 190602-32	si	2.2	29	5.76	0.44	0.93	1.03	18.29	6.89	2.71	0.40	0.15	468
CNF 02-322-A	sh								19.29		0.55	0.05	
CNF 02-326DP	sh								9.69		0.86	0.10	
CNF CN63,5	sh								35.57		0.51	0.03	
CNF 180602-04	sh								38.02		0.51	0.03	
CNF 180602-40	sh								21.80		0.56	0.05	
CNF 180602-58	sh								28.66		0.16	0.03	
CNF 190602-02	sh								25.87		0.35	0.04	
CNF 190602-14	sh								24.94		0.50	0.04	
CNF 190602-39	sh								21.98		0.42	0.05	
CNF 190602-45	sh								15.52		0.27	0.06	

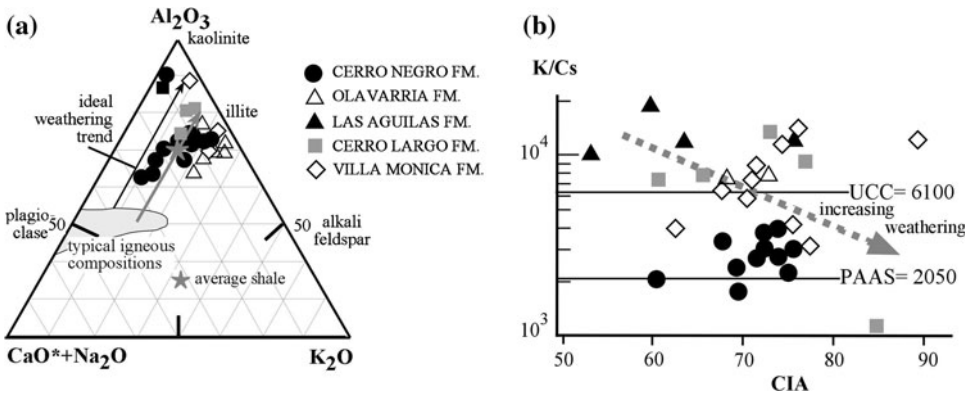

Fig. 3 **a** CIA and ACNK trivalent diagram (after Fedo et al. 1995). **b** K/Cs versus CIA to quantify chemical weathering (after McLennan et al. 1993)

Negro Formation with values around 70 (Table 1). The latter formation follows a clear trend, different from all other formations (Fig. 3a). K/Cs ratios scatter for the rocks of the Sierras Bayas Group strongly and point to different influences of detritus and/or different weathering histories (Fig. 3b). In contrast, the rocks of the Cerro Negro Formation display values between typical UCC (after McLennan et al. 2006) and the PAAS (Post-Archaean Australian Average shale, Taylor and McLennan 1985).

Trace element composition

Rare earth elements (REE)

Samples of the Villa Mónica Formation show a large variation in REE concentration (Fig. 4a and b), including sample T6EP 35.5, which is extremely enriched in REE, reflecting a prominent influence of unrecycled magmato-metamorphic detritus and the high amount of pyrophyllite-illite (Poiré et al. 2005). The quartz-rich samples are diluted in REE, where the few clay mineral-rich rock have nearly PAAS-like (Post-Archaean Australian average Shale, after Nance and Taylor (1976); representing a UCC composition) pattern. These are comparable to those of the rocks of the Las Águilas Formation (Fig. 4a, d). The samples of the Cerro Negro Formation are strongly diluted in REE, partly close to the detection limit; hence, they show sometimes an irregular pattern for a quartz-arenite (Fig. 4c). Only three samples contain higher REE concentration, as such as their patterns are similar to that of PAAS, but the concentrations are significantly lower (Figs. 4, 1b data repository). The Olavarría Formation samples are variable and their average pattern is clearly enriched in all REE in comparison with PAAS with one sample, PEL INTRACL, which displays a flat and strongly enriched REE pattern (Fig. 4d). The samples of the Cerro Negro Formation plot in two larger groups (in Fig. 4a, e averaged to typical UCC represented by PAAS). One group is depleted in REE, because they are quartz-richer and the second group is mostly enriched in REE compared to PAAS (Fig. 4e). La_N/Yb_N ratios are nearly in all samples above typical UCC value (~6; Table 1; McLennan et al. 1993). Two samples of the Olavarría Formation have a rather flat pattern (03-331; PEL INTRACL) and such values are characteristic for the Cerro Negro Formation (average 6.52; Table 1) with nearly 50% of the samples below 6. Eu/Eu* values are in most of the samples below 1 and point to the relative absence of plagioclase (McLennan et al. 1990), as supported by our petrographic observations and XRD data. Some quartz-arenites show higher Eu/Eu* values because of the Eu concentrations close to the detection limit of the method. Such untypical values for quartz-arenites are in italics in Table 1. Ce/Ce* values can give insight to mainly post-depositional mobility of REE, as Ce/Ce* values are negative if reducing environmental conditions dominated, and positive if oxidising conditions prevailed (e.g. Milodowski and Zalasiewicz 1991; McDaniel et al. 1994; Dobrzinski et al. 2004). Values significantly above 1.0 can only be observed at the top of the Cerro Largo Formation and in the samples of the Las Águilas Formation, and the samples of the Villa Mónica Formation show a definite trend from lower values to those close to 1 (Table 1).

An estimation of the composition of the sources of the sedimentary rocks can be made using the Zr/Ti vs. Nb/Y ratio plot (Winchester and Floyd 1977; Fralick 2003; Lacassie et al. 2006; Van Staden et al. 2006; Bertolino et al. 2007), as these elements are immobile (Fig. 5). The Villa Mónica Formation is characterised by the highest Nb/Y ratios pointing to an alkaline compositional trend. The Cerro Largo Formation samples display a large spread from alkaline to non-alkaline compositions with always relatively high Zr/Ti ratios. The overlying rocks of the Las Águilas Formation display a rhyolitic composition, while the samples of the Olavarría Formation scatter with lower Zr/Ti ratios. However, the samples of the Cerro Negro Formation indicate a clear change with a trend to an andesitic composition.

Trace elements like high field strength elements Th, Sc and Zr and REE are particularly useful for provenance

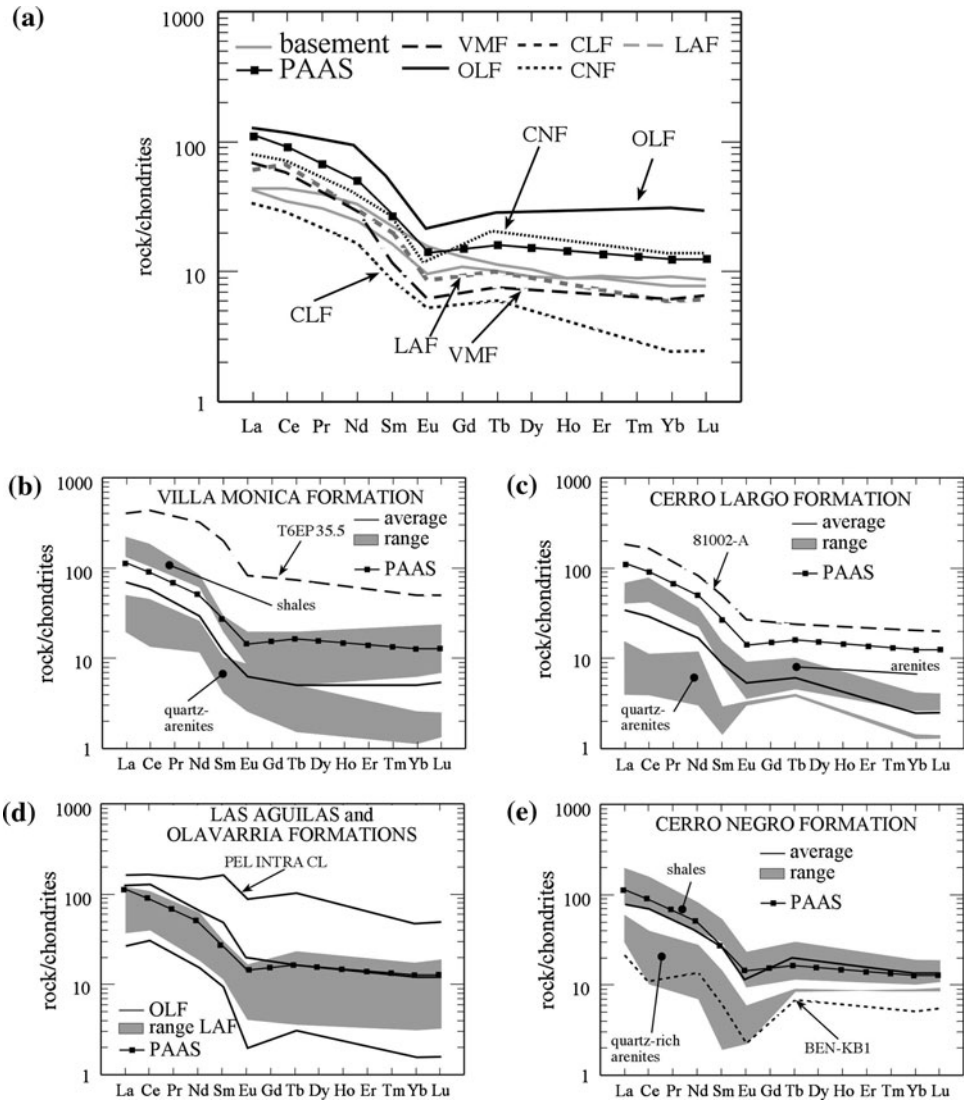

Fig. 4 **a** REE pattern for averages of each formation are shown compared to samples of the underlying basement. **b**–**e** Detailed REE pattern for the five formations normalised to chondrite (after Taylor and McLennan 1985). **b** Villa Mónica Formation. **c** Cerro Largo Formation. **d** Olavarría and Las Águilas Formations. **e** Cerro Negro Formation. Post-Archaean Average Shale (*PAAS* Post-Archaean Australian Average Shale; after Taylor and McLennan 1985) is shown for comparisons. (*VMF* Villa Mónica Formation, *CLF* Cerro Largo Formation, *LAF* Las Águilas Formation, *OLF* Olavarría Formation, *CNF* Cerro Negro Formation, *PAAS* Post-Archaean Australian Average Shale and chondritic normalisation after Taylor and McLennan 1985)

analysis as they are insoluble and usually immobile under surface conditions, thus preserving characteristics of the source rocks in the sedimentary record (e.g. Taylor and McLennan 1985; Bhatia and Crook 1986; McLennan et al. 1990, 1993, 2003). Figure 6a shows trends for the successions using Th/Sc versus Zr/Sc ratios. The samples of the Villa Mónica Formation are all reworked with some samples having Zr/Sc ratios from 30 to 100. Overlying quartz-arenites of the Cerro Largo Formation pretend to be stronger recycled, but have mostly similar Zr/Sc ratios. One sample (81002-H) is enriched in Sc over Th and Zr; therefore, it plots towards less fractionated sources. This sample is fine-grained and might reflect a single layer composed of less fractionated detritus, which is confirmed by a relatively flat REE pattern ($La_N/Yb_N = 5.63$; Table 1). Samples from the Las Águilas Formation are composed of recycled material and plot partly similar to

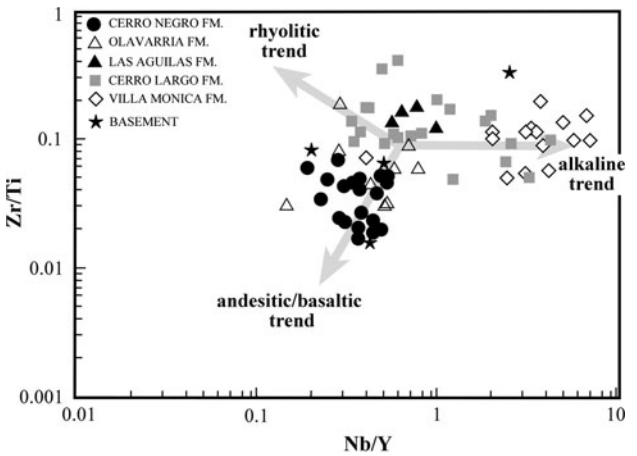

Fig. 5 Composition of the clastic rocks of the Sierras Bayas Group and the Cerro Negro Formation from the Tandil System (after Winchester and Floyd 1977)

some rocks of the two former formations. The three samples of the Olavarría Formation show, in contrast, a wide range. One sample, PELINTRA displays a close affinity to some samples of the overlying Cerro Negro Formation. Rocks of the latter are definitely composed of different source rock material. These samples show a typical UCC composition (white star in Fig. 6a) and nearly 50% of the rocks indicate a dominant influence of less fractionated material than UCC, with Zr/Sc ratios < 10 and Th/Sc < 0.8.

A similar geochemical trend can be observed in Fig. 6b, where La/Sc is plotted against Ti/Zr. The samples of the Villa Mónica Formation comprise two fractions, one sample group point towards an old crustal component, while a second group of samples has lower La/Sc ratios, but is definitely reworked or related to felsic source material as low Ti/Zr ratios show. A similar spread in La/Sc ratios is recorded in the Cerro Largo and Las Águilas Formations. The rocks of the Olavarría Formation have relatively similar low La/Sc ratios (around 4) but variable Ti/Zr values, which indicates different portions of felsic (indicated by Zr concentrations) and a less fractionated sources (expressed by Ti concentrations) in their detrital mix. The rocks of the Cerro Negro Formation are again different as their high Ti/Zr ratios correlate with low La/Sc ratios. Figure 6c further illustrates the different character of the samples from the Cerro Negro Formation in comparison with those of the Sierras Bayas Group. The latter plot shows the clear affinity to a passive margin setting (according to the diagram), while the overlying rocks of the Cerro Negro Formation would point to a continental arc (Bhatia and Crook 1986; McLennan et al. 1993); however, these trends need cautious analysis before interpreting (see below). Only very few samples of the Sierras Bayas Group plot similar to the younger Cerro Negro Formation. The combination of these plots demonstrates the main two source components for the Cerro Negro Formation: (a) a source less fractionated than typical UCC and (b) a source, which reflects UCC.

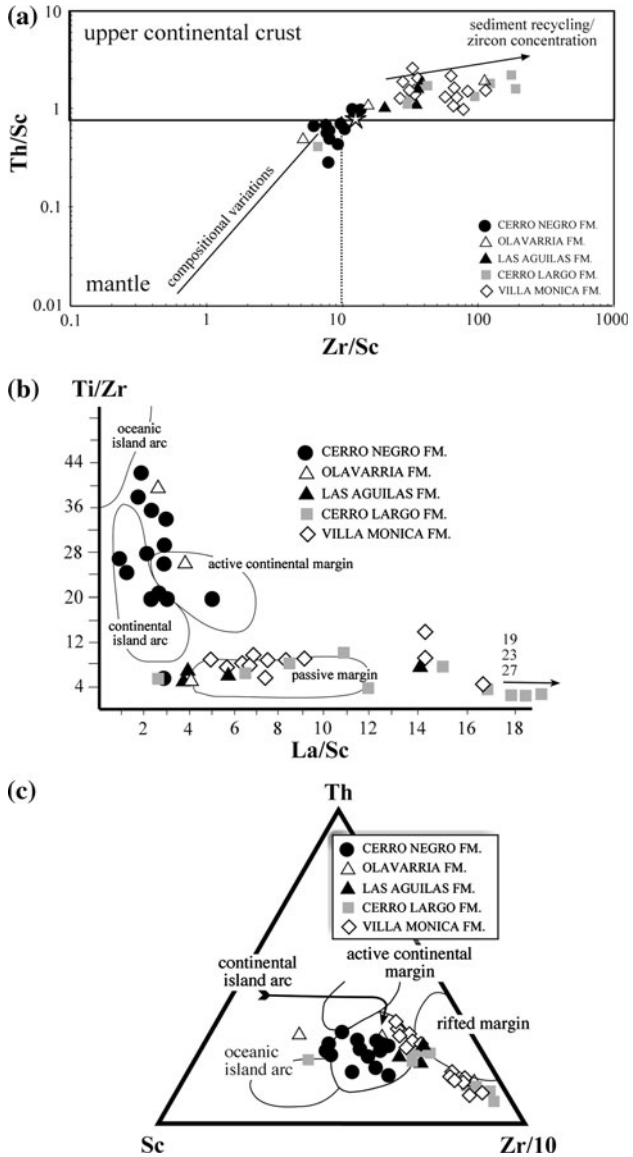

Fig. 6 **a** Th/Sc vs. Zr/Sc plot to reveal the source area composition of the rocks of the Sierras Bayas Group and Cerro Negro Formation (after McLennan et al. 1990). **b** Ti/Zr versus La/Sc (after Bhatia and Crook 1986) to determine the tectonic setting of the source rocks. **c** Trivalent plot of Th–Sc-Zr/10 (Bhatia and Crook 1986), which excludes LREE for provenance interpretations

Implication of the provenance data

Petrographic studies have shown that the main source of the Sierras Bayas Group was composed of quartz-rich, sedimentary and (meta-)sedimentary rocks including phyllites, gneisses, as well as quartzites (granulites); rock types which comprise the basement of the Río de la Plata craton (e.g. Rapela et al. 2003). The amount of plutonic debris is difficult to estimate as felsic plutonic lithoclasts were not identified and most probably decayed to quartz and microcline. A significant amount of detritus, derived from alkaline meta-igneous rocks, is deposited only in the Villa Mónica Formation, but rare in the Cerro Largo Formation (Fig. 5). The rocks of the Cerro Negro Formation, in contrast, comprise a significant amount of volcanic debris and for the first time in the stratigraphic succession sedimentary lithoclasts. Thin volcaniclastic beds are associated with wackes and lithoclast-rich arenites. This indicates the clear change in provenance above the regional unconformity underlying the Cerro Negro Formation. Occasionally, a geochemically less fractionated source can be observed in some layers of the Sierras Bayas Group with sample PETINTRA of the Olavarría Formation and 81002-H of the Cerro Largo Formation. The latter is a wacke and

the former a clay-rich rock with clayey reworked intraclasts and a pyroclastic texture.

The geochemical information can be compared with detrital zircon ages known from some formations of the Sierras Bayas Group and Lower Palaeozoic rocks. The results are schematically compared in Fig. 7 and compiled from Rapela et al. (2007), Gaucher et al. (2008) and Van Staden et al. (2010). Gaucher et al. (2008) present data from a single rock sample of the Villa Mónica Formation directly overlying basement rocks. The data are uniform and date the underlying meta-igneous rock with a Palaeoproterozoic age (Cingolani et al. 2002), indirectly. The other sample of the Sierras Bayas Group (Cerro Largo Formation) shows nearly a similar detrital zircon signature with only few Mesoproterozoic zircons (1.1–1.2 Ga; Rapela et al. 2007). Quartz-arenites of the Cerro Largo Formation were stronger reworked than those of the older Villa Mónica Formation (Figs. 5, 6), which might be responsible for the slightly more variable detrital zircon age spectra regarding post-Mesoproterozoic ages and a significant Palaeoproterozoic and Late Archaean source component (Rapela et al. 2007). However, these data are not representative for the composition of the Río de la Plata craton but might shed light on the basin evolution and sediment transport characteristics during deposition of the

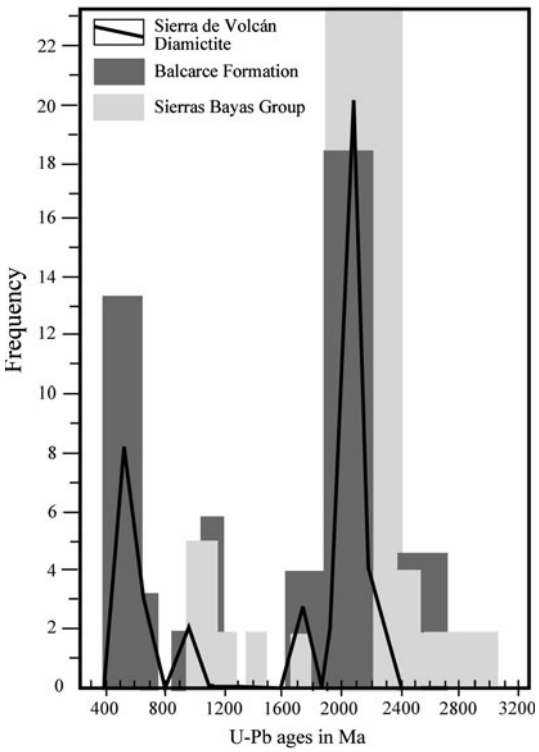

Fig. 7 Schematic detrital zircon age distribution for deposits in the Tandilia area (data from Rapela et al. 2007; Gaucher et al. 2008; van Staden et al. 2010)

Sierras Bayas Group (see below). However, the unconformity between the Villa Mónica and Cerro Largo Formations (Poiré 2004; Gómez Peral 2008; Fig. 2a) would support changing basin conditions, with a redesign of the basin shape and the consequential possibility to erode a wider range of rock types. This would explain the different geochemical fingerprint for Nb/Y ratios for the rocks of the Villa Mónica Formation in comparison with those of the Cerro Largo Formation (Fig. 5). The shift to less alkaline rocks as the dominant source component is compelling. It remains unclear why no Neoproterozoic zircons arrived in the recycled quartz-arenites of the Cerro Largo Formation. Palaeocurrents changed from eastern (Villa Mónica Formation) to southern directed ones in the Cerro Largo Formation, hence the central and western region of Uruguay could have had functioned as a source, which would explain the occurrence of Palaeoproterozoic and older zircons. However, different tectonic models report magmatic activity during the Ediacaran (e.g. Basei et al. 2000; Oyhantçabal et al. 2009), and zircons of such an age were discovered in the Neoproterozoic rocks of the Barriga Negra Formation in central Uruguay (Blanco et al. 2009); they should therefore also be deposited in the Cerro Largo Formation. An explication would be the existence of a palaeo-high between the Argentinean and the Uruguayan deposits, which exposed older basement material and blocked sediment supply from Uruguay. Large areas of the Río de la Plata craton around the Tandilia area is covered by post-Palaeozoic sediments, and it is therefore plausible that Palaeoproterozoic and Archaean basement material was exposed during Neoproterozoic and Palaeozoic times (Fig. 7). However, petrographically comparable recycled quartz-arenites have been deposited in the Tandil area in the Ordovician to Silurian Balcarce Formation (Zimmermann and Spalletti 2009; Van Staden et al. 2010). Their detrital zircon ages cover a wide range of ages from Ordovician to Late Archaean with peaks during the Ediacaran (Rapela et al. 2007; Van Staden et al. 2010; Fig. 7). This implies that different depositional environments or basin morphologies with unalike catchment areas existed during deposition of these two quartz-rich sediments.

At the time of deposition of the Cerro Negro Formation, and partially the Olavarría Formation, the detritus changes and the influence of less fractionated material is often recognisable (see Figs. 5, 6). The age of the detritus is unknown and it remains speculative if the volcaniclastic debris was erupted synsedimentary or earlier. However, volcanic or volcaniclastic rocks are not described so far from the Sierras Bayas Group or the local basement. Geochemical proxies, like relatively flat REE pattern ($La_N/Yb_N < 6$; Fig. 1d data repository; Table 1), and a continental arc provenance for the rocks (Fig. 6b and c) are not visible in the entire formation, but represent the general

geochemical trend in this formation. The detritus is therefore composed of felsic and less fractionated source(s).

Selected trace elements and their ratios can be used to test a possible arc signature for most of the samples of the Cerro Negro Formation (after Floyd and Leveridge 1987; McLennan et al. 1990, 1993; Zimmermann et al. 2009a). In Table 2, geochemical values for those samples indicating an arc derivation for detrital mixes are shadowed in grey. Most of the samples display a number of proxies of a continental arc component mixed with a felsic source, independent of grain size (Tables 1 and 2). Moreover, volcaniclastic samples show a stronger arc-related signature (e.g. CN 60.2; 180602-48; Table 2) than others. However, Eu/Eu* values are all below 1 and point to a lack of abundant plagioclase in the source and Zr/Sc ratios are often slightly higher than expected in typical immature arc systems (McLennan et al. 1993), where limited reworking of the detritus and rapid burial dominates. The low Eu/Eu* values can be explained by a significant influence of felsic sources, derived from the basement, into the detrital mix of the formation, which also accounts for higher Zr concentration and overprints the high Sc concentrations, which are up to twice the typical value for UCC (Table 1). Absolute concentrations of the compatible elements Ti, Nb and Ta are often used to determine an arc derivation in magmatic rocks (Hofmann 1988, 1997). In typical continental arc environments, such a trend is visible in volcaniclastic sedimentary rock (Floyd and Leveridge 1987) and observed in an Ordovician arc environment in northwest Argentina (Zimmermann and Bahlburg 2003; Zimmermann et al. 2009a). Tectonic processes in foreland basins or retro-arc basin could exhume basement material, including mafic sources, as observed in Ordovician arc terranes and today in northwest Argentina, with a trend of decreasing geochemical arc signals away from the subduction zone (Bahlburg 1998; Zimmermann and Bahlburg 2003; Zimmermann et al. 2009a). A distal position to the proposed active continental margin to the west and south of the Río de la Plata craton (Cawood 2005; Chew et al. 2008) could explain the typical UCC (after McLennan et al. 2006) and enriched Nb (~20 ppm) and Ti (>1%) values in some samples. The relative lack of plagioclase and the occurrence of quartz-rich sedimentary and metamorphic lithoclasts in the rocks of the Cerro Negro Formation point to a distal position to an active margin on the continental side of the retro-arc basin or in a retro-arc foreland-basin (Fig. 8). Thus, the Cerro Negro Formation represents most probably a mixing of three source types of probably different ages: (a) one less fractionated resembling arc rocks, (b) a mafic and (c) felsic source. The rock succession is sporadically affected by kaolinisation and precipitation of hydrothermal rutile (Dristas and Frisicale 1996; Zimmermann and Spalletti 2009), which accounts for the Nb, Ta and Ti budget in a sedimentary rock (Zack et al. 2002). This process might have added some Nb and Ti and also affected the Ti/Zr ratios (Table 2; Figs. 4, 6b). However, lower Ti/Zr ratios would not change the main character of the Cerro Negro Formation, more samples would plot in the continental arc field (Fig. 6b). The age for the Cerro Negro Formation based on detailed biostratigraphy

Table 2 Arc (ARC*) defining trace element abundances and ratios (compiled from Floyd and Leveridge 1987; McLennan et al. 1990, 1993, 2003)

Sample		SiO_2	La/Sc	Th/Sc	Zr/Sc	Ti/Zr	Eu/Eu*	LaN/YbN	TiO_2	Nb	Ta
02-322	CNF	68.5	**2.20**	0.89	18.98	19.34	0.58	**5.53**	0.70	14.50	0.8
02-324	CNF	60.7	**2.33**	**0.68**	14.24	**26.47**	0.57	6.14	0.81	15.50	1
02-326B	CNF	62.9	**0.63**	**0.69**	14.37	**24.96**	0.57	**3.10**	1.05	20.3	1.2
CN 66,45	CNF	56.1	**2.41**	**0.63**	**8.16**	**34.85**	0.63	7.78	0.75	16.7	
CN 60,2	CNF	57.9	**2.29**	**0.58**	**8.18**	**42.41**	0.56	6.36	0.81	15.7	1.1
CN 66,15	CNF	51.9	3.16	**0.78**	**6.39**	**39.81**	0.45	9.70	0.93	18.8	1.3
180602-21	CNF	70.5	**2.70**	1.00	19.75	**20.43**	0.48	**5.21**	**0.67**	13.2	
180602-29	CNF	56.4	3.07	0.85	**10.09**	**28.05**	0.54	8.66	0.89	17.5	
180602-48	CNF	55.5	**2.53**	0.81	**8.20**	**32.65**	0.59	8.66	0.88	17.2	
190602-06	CNF	66.0	3.11	0.97	19.03	18.66	0.49	6.36	**0.61**	13.2	
190602-18	CNF	63.1	3.07	0.80	12.60	**25.70**	0.46	7.88	0.74	15.6	
190602-53	CNF	65.0	**2.38**	**0.55**	**8.72**	**38.65**	0.47	7.66	0.80	16.3	
190602-57	CNF	66.3	**2.90**	1.00	20.40	**21.83**	0.65	**5.94**	0.74	14.7	1.4
190602-32	CNF	64.4	**2.71**	1.03	18.29	6.89	0.44	**5.76**	**0.32**	**11.5**	
ARC*			<3	<0.81	<10	>20	1.00	<6	<0.68	<12	<1

Bold contain values, which point to an arc derivation. *N* chondritic normalisation, *CLF* Cerro Largo Formation, *OLF* Olavarría Formation, *CNF* Cerro Negro Formation

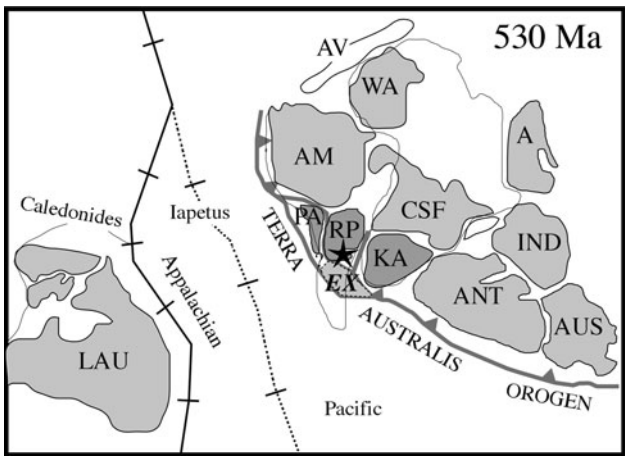

Fig. 8 Palaeotectonic model (adapted from Rapela et al. (1998) and Cawood (2005)) for the time of subduction along the southern margin of Gondwana (latest Ediacaran to lowermost Cambrian) during deposition of the Cerro Negro Formation according to biostratigraphic evidence. *LAU* Laurentia, *AV* Avalon, *WA* West Africa, *AM* Amazonia, *RP* Rio de la Plata craton, *PA* Pampia, *EX* exotic terrane (Patagonia, Western Pampean belt), *KA* Kalahari craton, *CSF* Congo-São Francisco craton, *ANT* Antarctica, *AUS* Australia, *IND* India, *A* Arabia; the star represents the study area)

(Gaucher and Poiré 2009a) allows in classifying the rocks as deposited during the end of the Uppermost Ediacaran.

Basin evolution

The erosion of the directly underlying rocks into small-scale basins initiated the evolution of the Sierras Bayas basin. This can be demonstrated by the similarity of the alkaline chemical character (Fig. 5) of the Villa Mónica Formation and underlying basement rocks (Pankhurst et al. 2003) and the uniform zircon population of both (Cingolani et al. 2002; Gaucher et al. 2008). However, during the evolution of the basin, detrital material was successively reworked and likely some older sources could have been transported from other areas into the basin. The origin of Mesoproterozoic zircons is not clear. Various authors argue that the absence of Mesoproterozoic zircons is a discriminating character for the Río de la Plata craton on its eastern margin (Gaucher et al. 2008; Blanco et al. 2009). However, Mesoproterozoic sources could have been buried since the Earliest Neoproterozoic, or eroded into another not anymore preserved earlier sedimentary cycle. Alternatively, palaeocurrents and sorting during transport could have sorted this component and deposited in another facies in this basin, not found so far. Additionally, often sampling techniques may be decisive in losing a certain source component (Andersen 2005; Zimmermann 2010). So, it is possible that local Mesoproterozoic source rocks had been exposed around the Sierra Bayas basin. However, any further speculation in this regard is still premature based on the few zircons per sample measured in all samples used for interpretation (Andersen 2005).

The erosional surface above the Villa Mónica Formation, which is marked by brecciated and diamictitic rocks and a karst surface, together with its abundant Cryogenian stromatolites (Poiré 1989, 1993) and stronger diagenetic overprint compared to the following Cerro Largo Formation (Gómez Peral 2008), points to a clearly older age for the former compared to the overlying rocks (Fig. 2a). Moreover, we can observe an obvious change in provenance information from the Villa Mónica Formation to the Cerro Largo Formation. Nearly primary C–O isotope excursions in the Villa Mónica Formation allow to interpret a Cryogenian age (Gómez Peral et al. 2007) as the data would fit into secular C curves (Halverson et al. 2010) for a pre-Ediacaran age. The overlying sedimentary succession, beginning with the Cerro Largo Formation, is therefore classified as Ediacaran and represents a different basin cycle.

Even though the main trend towards an older felsic component is visible in the Cerro Largo Formation (Fig. 6c), influence of intermediate or less fractionated material (Fig. 6; Table 1) occurred sporadically in some samples (81002-H) and later in the Olavarría Formation (PELINTRACL). Previous work interpreted that the regional palaeotectonic framework was dominated by large-scale subduction of oceanic crust to the east of eastern Argentina during the later Ediacaran to consume the Adamastor Ocean (e.g. Stanistreet et al. 1991) or other newly defined oceanic basins. This proposed tectonic process is not recorded tectonically in the rocks of the Sierras Bayas Group, but might be expressed by these sporadic influences. This could support the interpretation that only minor oceanic crust was formed and subducted during the Neoproterozoic (Basei et al. 2008).

During the end of the Ediacaran, the detrital composition changed rigorously with the deposition of the Cerro Negro Formation. This Uppermost Ediacaran formation (Gaucher and Poiré 2009a) comprises different lithotypes and volcaniclastic rocks intercalated with pyroclastites with an arc signature. These characteristics are absent in proposed to be equivalent aged deposits in central Uruguay (Gaucher et al. 2005; Blanco et al. 2009). Here, the proposed volcanic arc is subject of a variety of recent different palaeotectonic models and related to Pan-Brazilian tectonic events, but so far not identified in Neoproterozoic sedimentary successions of the Río de la Plata craton (e.g. Basei et al. 2008; Gaucher et al. 2008; Oyhantçabal et al. 2009). If this volcanic arc would have been the main source for the sediments in the Cerro Negro Formation then the model by Gaucher et al. (2008) and Blanco et al. (2009) needs to be revised, in which the suggested magmatic arc

was still separated from the Río de la Plata craton during the Ediacaran. This would reason the absence of volcaniclastic debris in Ediacaran deposits in central Uruguay. In contrast, the palaeotectonic models by Basei et al. (2008) and Oyhantçabal et al. (2009) would allow for a Pan-Brazilian arc source based on our age constraints of the Cerro Negro Formation.

Although an active continental margin for southern Gondwana is proposed (Cawood 2005; Gregori et al. 2004; Chew et al. 2008), no arc-related sedimentary rocks are so far detected in Argentina. An active continental margin is proposed on the western and southern margin of the craton (Gregori et al. 2004; Chew et al. 2008) and supports the Terra Australis orogen (Fig. 8). The Cerro Negro Formation is the first deposit, which could reflect this model for the Río de la Plata Craton. If so, we can interpret that the Cerro Negro Formation was deposited in a retro-arc foreland or retro-arc basin related to the Terra Australis Orogen (Cawood 2005; Fig. 8). The actual arc must then be located further south on the same Río de la Plata Craton or is represented by a separated arc terrane (Fig. 8). The provenance of the Cerro Negro Formation points to three significant source types like (a) felsic, (b) mafic and (c) arc derived (Table 2) ones, which are observed in ancient retro-arc (foreland) basins (e.g. Zimmermann and Bahlburg 2003). Palaeocurrents are scarce in the Cerro Negro Formation ($n = 4$) and cannot be representative for a main source location, as the interpretation of a retro-arc or retro-arc foreland basin allows for a variety of possible palaeocurrent pattern. Therefore, a regional collection of palaeocurrent data, as for the overlying Balcarce Formation exercised (compilation in Zimmermann and Spalletti 2009), would be necessary. Interesting enough, volcaniclastic debris is observed in Neoproterozoic rocks of similar age (Praekelt et al. 2008) at the southern margin of the Kalahari craton, which could have been similarly affected by this same active margin (Naidoo et al. 2006; Naidoo 2008; Zimmermann 2009). Therefore, it is possible to suggest that during the latest Ediacaran, the Tandil area was related to a similar palaeotectonic setting as deposits along the southern margin of the Kalahari craton and is, in its evolution, not related to basins to its north and northeast.

Therefore, the basin evolution in the Tandilia area and its provenance information do not reflect the proposed palaeotectonic events like rift, drift and collisional events.

Hence, the geochemical and isotope geochemical signature of the Sierras Bayas Group reflects relatively small basins, while in contrast, the Cerro Negro Formation and the overlying Palaeozoic Balcarce basin received sediment from a larger catchment area, which is mirrored in the provenance data (Rapela et al. 2007; Zimmermann and Spalletti 2009; Van Staden et al. 2010; this study). This points to a rigorous change in the palaeotectonic setting. This basin evolution is compellingly similar to southern South Africa where smaller Neoproterozoic basins are covered by large Lower Palaeozoic basins and might point to one large craton cover sequence (e.g. Theron 1972; Zimmermann et al. 2009b; Fourie 2010; Van Staden et al. 2010).

The rocks of the Sierras Bayas Group and the Cerro Negro Formation are also devoid of any detritus related to glacial events and clastic glacial deposits beyond doubt (e.g. Poiré 2004). A glacial diamictite (Spalletti and Del Valle 1984), proposed to be of Neoproterozoic age (Zimmermann et al. 2005; Pazos et al. 2008), revealed Ordovician detrital zircons (Van Staden et al. 2010). The sedimentary rocks of the Tandil area also do not reflect extreme temperature changes as the lithostratigraphy contains only warm water carbonates according to interpretation of their C–O isotope signature (Gómez Peral et al. 2007) together with the occurrence of stromatolites and *Cloudina* sp.. Hence, correlation on a regional or global scale based on occurring diamictites or C–O chemostratigraphy, which may reflect elsewhere such dramatic climate changes, shall not be executed for the Sierras Bayas Group and the Cerro Negro Formation. It is possible that the exposed sedimentary successions in the Tandilia area indicate other time periods than the suggested glacial events. Knowingly, the correlation of glacial diamictites and related carbonate rocks is generally hampered by the relative short extent of these events during the Neoproterozoic (see the discussion by van Loon 2000, 2008).

Conclusions

The provenance of the Neoproterozoic Sierras Bayas Group and the overlying Uppermost Ediacaran Cerro Negro Formation of the Tandilia System in eastern Argentina revealed a regional unique basin evolution from small-scale depositional areas to an arc-related basin. Recycled clastic rocks were deposited with successions of carbonates (Sierras Bayas Group) between c. 800 and 548 Ma. The detritus of the Cerro Negro Formation comprises volcanic and mafic debris possibly related to an active continental margin fringing Gondwana in the south during the latest Ediacaran and Early Cambrian (Terra Australis Orogen). The Cerro Negro Formation is, therefore, based on our current knowledge, explained as a marine retro-arc foreland basin or the continental margin of a retro-arc basin, deposited during the Uppermost Ediacaran, based on well-constrained microfossil fauna, and a basal regional unconformity expressed as a karst horizon dated in Paraguay and Namibia as young as c. 555 Ma. Comparable deposits to the Cerro Negro Formation in composition and age can be found at the southern margin of the actual Kalahari craton.

The lack of metamorphism and deformation is the substantial geological difference of the rocks of the Sierras Bayas and Cerro Negro Formation compared to all other Neoproterozoic deposits with an assumed similar age in southwest Gondwana, besides the Nama Group. This offers the possibility in interpreting a different geological history for this area as being related to geological processes further to the south of the basin rather than with those to its northeast. Revealing the provenance information in these rocks adds important information in regard to the evolution of southwestern Gondwana during the Ediacaran, and combined with other new data offers the chance in developing for a less debated palaeotectonic model.

Acknowledgments Fieldwork was supported by funds of the CONICET and Cemento Avellaneda S.A. wherefore DGP and LPG are thankful. XRF analyses were executed at the University of Johannesburg. Statoil and Marathon Norge supported other analytical work. We are grateful to S. Siegesmund and M.A.S. Basei to be invited to this special volume. We thank V.A. Janasi and an anonymous reviewer for their very helpful and thoughtful comments, which improved the manuscript.

References

Andersen T (2005) Detrital zircons as tracers of sedimentary provenance: limiting conditions from statistics and numerical simulation. Chem Geol 216:249–270

Andreis RR, Zalba PE, Iñiguez Rodríguez AM (1992) Paleosuperficies y Sistemas Depositacionales en el Proterozoico Superior de Sierras Bayas, Sierras Septentrionales, Pcia. Buenos Aires, Argentina. In: IV Reunión Argentina de Sedimentología, La Plata, Argentina, Proceedings, vol 1, pp 283–290

Bahlburg H (1998) The geochemistry and provenance of Ordovician turbidites in the Argentinian Puna. In: Pankhurst RJ, Rapela CW (eds) The Proto-andean margin of gondwana. Geol Soc London Spec Publ 142:127–142

Barrio CA, Poiré DG, Iñiguez MA (1991) El contacto entre la Formación Loma Negra (Grupo Sierras Bayas) y la Formación Cerro Negro, un ejemplo de palaeokarst, Olavarría, provincia de Buenos Aires. Revista de la Asociación Geológica Argentina 46:69–76

Basei MAS, Siga O Jr, Masquelin H, Harara OM, Reis Neto JM, Preciozzi Porta F (2000) The Dom Feliciano Belt and the Rio de la Plata Craton: tectonic evolution and correlation with similar provinces of southwestern Africa. In: Cordani UG, Milani EJ, Thomas Filho A, Campos DA (eds) Tectonic evolution of South America. 31st Intern Geol Congress, Rio de Janeiro, pp 311–334

Basei MAS, Frimmel HE, Nutman AP, Preciozzi F, Jacob J (2005) A connection between the Neoproterozoic Dom Feliciano (Brazil/Uruguay) and Gariep (Namibia/South Africa) orogenic belts—evidence from a reconnaissance provenance study. Prec Res 139:195–221

Basei MAS, Frimmel HE, Nutman AP, Preciozzi F (2008) West Gondwana amalgamation based on detrital zircon ages from Neoproterozoic Ribeira and Dom Feliciano belts of South America and comparison with coeval sequences from SW Africa. Geol Soc London Spec Publ 294:239–254

Bertolino SRL, Zimmermann U, Sattler F (2007) Mineralogy and geochemistry of bottom sediments from water reservoirs in the vicinity of Córdoba, Argentina: environmental and health constraints. Appl Clay Sci 36:206–220

Bhatia MR, Crook KAW (1986) Trace elements characteristics of graywackes and tectonic setting discrimination of sedimentary basins. Contrib Mineral Petrol 92:181–193

Blanco G, Rajesh HM, Gaucher C, Germs GJB, Chemale F Jr (2009) Provenance of the Arroyo del Soldado Group (Ediacaran to Cambrian, Uruguay): implications for the palaeogeographic evolution of southwestern Gondwana. Prec Res 171:57–73

Cawood PA (2005) Terra Australis Orogen: rodinia breakup and development of the Pacific and Iapetus margins of Gondwana during the Neoproterozoic and Palaeozoic. Earth Sci Rev 69:249–279

Celesia N, Rapalini AE, Geuna SE, Singer SE (2008) Modelado magnetométrico del intrusivo básico de la Sierra de los Barrientos, Provincia de Buenos Aires. XVII Congreso Geológico Argentino, Actas 3:1075–1076

Chew DM, Magna T, Kirkland CL, Miskovic A, Cardona A, Spikings R, Schaltegger U (2008) Detrital zircon fingerprint of the Proto-Andes: evidence for a Neoproterozoic active margin? Precam Res 167:186–200

Cingolani C, Bonhomme MG (1982) Geochronology of La Tinta Upper Proterozoic sedimentary rocks, Argentine. Precam Res 18:119–132

Cingolani C, Rauscher R, Bonhomme MG (1991) Grupo La Tinta (Precámbrico y Palaeozoico inferior) Provincia de Buenos Aires, República Argentina: Nuevos Datos Geocronológicos y Micropalaeontológicos en las Sedimentitas de Villa Cacique, Partido de Juárez. Revista YPFB, Bolivia 12:177–191

Cingolani CA, Hartmann LA, Santos JOS, McNaughton NJ (2002) U–Pb SHRIMP dating of zircons from the Buenos Aires Complex of the Tandilia belt, Rio de la Plata craton, Argentina. In: XV Congreso Geológico Argentino, El Calafate, Actas, CD-ROM

Dobrzinski N, Bahlburg H, Strauss H, Zhang Q (2004) Geochemical climate proxies applied to the Neoproterozoic glacial succession on the Yangtze Platform, South China. In: Jenkins G, McMenamin M, Sohl L, McKay C (eds) The extreme Proterozoic: geology, geochemistry and climate. Am Geophys Union Monograph Ser 146:13–32

Dristas JA, Frisicale MC (1984) Estudio de los yacimientos de arcilla del Cerro Reconquista, San Manuel, Sierras Septentrionales de la provincia de Buenos Aires. IX Congreso Geológico Argentino, San Carlos de Bariloche V:507–521

Dristas JA, Frisicale MC (1996) Geochemistry of an altered pyroclastic suite interbedded in the sedimentary cover of the Tandilia Area, Buenos Aires Province, Argentina. Zentr Geol Pal I:659–675

Drobe M, López de Luchi M, Steenken A, Wemmer K, Naumann R, Frei R, Siegesmund S (2010) Geodynamic evolution of the Eastern Sierras Pampeanas based on eochemical, Sm-Nd, Pb-Pb and SHRIMP data; this volume

Fedo CM, Nesbitt HW, Young GM (1995) Unravelling the effects of potassium metasomatism in sedimentary rocks and palaeosoils, with implications for palaeoweathering conditions and provenance. Geology 23:921–924

Floyd PA, Leveridge BE (1987) Tectonic environment of the Devonian Gramscatho basin, south Cornwell: framework mode and geochemical evidence from turbidite sandstones. J Geol Soc London 144:531–542

Fourie PH (2010) Provenance and palaeotectonic setting of the Devonian Bokkeveld Group, Cape Supergroup, South Africa; MSc thesis, University of Johannesburg, 148p

Fralick P (2003) Geochemistry of clastic sedimentary rocks: ratio techniques. In: Lentz DR (ed) Geochemistry of sediments and sedimentary rocks: evolutionary considerations to mineral-deposit-forming environments. Geol Assoc Can GEOText 4:85–104

Frimmel HE, Fölling PG (2004) Late vendian closure of the adamastor ocean: timing of tectonic inversion and syn-orogenic sedimentation in the Gariep Basin. Gondwana Res 7:685–699

Frimmel HE, Klötzli U, Siegfried P (1996) New Pb-Pb single zircon age constraints on the timing of the Neoproterozoic glaciation and continental break-up in Namibia. J Geol 104:459–469

Frisicale MC, Dristas JA (2000) Génesis de los niveles arcillosos de la Sierra de La Tinta, Tandilia. Revista de la Asociación Geológica Argentina 55:3–14

Gaucher C, Poiré DG (2009a) Biostratigraphy. Neoproterozoic-Cambrian evolution of the Río de la Plata Palaeocontinent. In: Gaucher C, Sial AN, Halverson GP, Frimmel HE (eds) Neoproterozoic-Cambrian tectonics, global change and evolution: a focus on southwestern Gondwana. Dev Precambrian Geol 16:103–114

Gaucher C, Poiré DG (2009b) Palaeoclimatic events. Neoproterozoic-Cambrian evolution of the Río de la Plata Palaeocontinent. In: Gaucher C, Sial AN, Halverson GP, Frimmel HE (eds) Neoproterozoic-Cambrian tectonics, global change and evolution: a focus on southwestern Gondwana. Dev Precambrian Geol 16:123–130

Gaucher C, Sprechmann P (2009) Neoproterozoic acritarch evolution. In: Gaucher C, Sial AN, Halverson GP, Frimmel HE (eds) Neoproterozoic-Cambrian tectonics, global change and evolution: a focus on southwestern Gondwana. Dev Precambrian Geol 16:319–326

Gaucher C, Poiré DG, Gómez Peral L, Chiglino L (2005) Litoestratigrafía, bioestratigrafía y correlaciones de las sucesiones sedimentarias del Neoproterozoico-Cámbrico del Cratón del Río de La Plata (Uruguay y Argentina). Latin Am J Sedimentolgy Basin Analysis 12:145–160

Gaucher C, Finney S, Poiré D, Valencia V, Grove M, Blanco G, Paoumukaghlian L, Peral L (2008) Detrital zircon ages of Neoproterozoic sedimentary successions in Uruguay and Argentina: insights into the geological evolution of the Río de la Plata Craton. Precam Res 167:150–170

Gómez Peral LE (2008) Petrología y Diagénesis de las unidades sedimentarias precámbricas de Olavarría, provincia de Buenos Aires. Facultad de Ciencias Naturales y Museo, Universidad Nacional de La Plata Tomo I: 327pp+tomo II: 292pp (PhD thesis)

Gómez Peral LE, Poiré DG, Strauss H, Zimmermann U (2007) Chemostratigraphy and diagenetic constraints on Neoproterozoic carbonate successions from the Sierras Bayas Group, Tandilia System, Argentina. Chem Geol 237:127–146

Gray RD, Foster DA, Goscombe B, Passchier C, Trouw AJ (2006) $^{40}Ar/^{39}Ar$ thermochronology of the Pan-African Damara Orogen, Namibia, with implications fortectonothermal and geodynamic evolution. Prec Res 150:49–72

Gregori DA, López VL, Grecco LE (2004) A Late Proterozoic-Early Palaeozoic magmatic cycle in Sierra de la Ventana, Argentina. J S Am Earth Sci 19:155–171

Gresse PG, von Veh MW, Frimmel HE (2006) Namibian (Neoproterozoic) to early cambrian sucessions. In: Johnson MR, Anhaeusser CR, Thomas RJ (eds) The Geology of South Africa, Council of Geoscience pp 395–420

Grey K, Calvert CR (2007) Correlating the Ediacaran of Australia. Geol Soc London Spec Publ 286:115–135

Halverson GP, Wade BP, Hurtgen MT, Barovich KM (2010) Neoproterozoic chemostratigraphy. Precam Res (in press)

Hofmann A (1988) Chemical differentiation of the Earth: the relationship between mantle, continental crust and oceanic crust. Earth Planet Sci Lett 90:297–314

Hofmann A (1997) Mantle geochemistry: the message from oceanic volcanism. Nature 385:219–229

Iñiguez Rodríguez AM (1999) La cobertura sedimentaria de Tandilia. In: Caminos R (ed) Geología Argentina. Subsecretaría de Miner5a de la Nación Servicio Geológico Minero Argentino Instituto de Geología y Recursos Minerales 29:101–106

Kawashita K, Varela R, Cingolani C, Soliani E Jr, Linares E, Valencio SA, Ramos AV, Do Campo M (1999) Geochronology and chemostratigraphy of "La Tinta" Neoproterozoic sedimentary rocks, Buenos Aires Province, Argentina. II South Amer Symp on Isotope Geology, Brazil 1:403–407

Lacassie JP, Herve F, Roser B (2006) Sedimentary provenance study of the post-Early Permian to pre-Early Cretaceous metasedimentary Duque de York Complex, Chile. Rev Geol Chile 33:199–219

McDaniel DK, Hemming SR, McLennan SM, Hanson GN (1994) Resetting of neodymium isotopes and redistribution of REEs during sedimentary processes: the Early Proterozoic Chelmsford Formation, Sudbury Basin, Ontario, Canada. Geoch Cosmochim Acta 58:931–941

McLennan SM, Taylor SR, McCulloch MT, Maynard JB (1990) Geochemical and Nd-Sr isotopic composition of deep-sea turbidites: crustal evolution and plate tectonic associations. Geochim Cosmochim Acta 54:2015–2205

McLennan SM, Hemming S, McDaniel DK, Hanson GN (1993) Geochemical approaches to sedimentation, provenance and tectonics. In: Johnsson MJ, Basu A (eds) Processes controlling the composition of clastic sediments. Geol Soc Am Spec Pap 284:21–40

McLennan SM, Bock B, Hemming SR, Horrowitz JA, Lev SM, McDaniel DK (2003) The roles of provenance and sedimentary processes in the geochemistry of sedimentary rocks. In: Lentz RD (ed) Geochemistry of sediments and sedimentary rocks: evolutionary considerations to mineral-deposit-forming environments. Geol Assoc Canada, GEOText 4:7–38

McLennan SM, Taylor SR, Hemming SR (2006) Composition, differentiation, and evolution of continental crust: constrains from sedimentary rocks and heat flow. In: Brown M, Rushmer T (eds) Evolution and differentiation of the continental crust. pp 92–134

Milodowski AE, Zalasiewicz JA (1991) Redistribution of rare earth elements during diagenesis of turbidite/hemipelagite mudrock sequences of Llandovery age from Central Wales. In: Morton AC, Todd SP, Haughton PDW (eds) Developments in sedimentary Provenance Studies, Geol Soc Am Spec Pap 57:101–124

Moore DM, Reynolds RC Jr (1989) X-Ray Diffraction and the Identification and Analysis of Clay Minerals. Oxford University Press, Oxford, p 329pp

Naidoo T (2008) Provenance of the neoproterozoic to early palaeozoic kango inlier, Oudtshoorn, South Africa. University of Johannesburg, MSc thesis; 261pp

Naidoo T, Zimmermann U, Germs GJB (2006) Provenance of the Neoproterozoic to Early Palaeozoic sedimentary rocks of the Kango Inlier, Saldania Belt (South Africa). Abstract, 17th Int Sed Congress, Fukuoka, Japan, O-300

Nance WB, Taylor SR (1976) Rare earth element patterns and crustal evolution—I. Australian Post-Archean sedimentary rocks. Geochim Cosmochim Acta 40:1539–1551

Nesbitt HW (2003) Petrogenesis of siliciclastic sediments and sedimentary rocks. In: Lentz DR (ed) Geochemistry of sediments and sedimentary rocks: evolutionary considerations to mineral-deposit-forming environments. Geol Assoc Canada GEOText 4:39–52

Nesbitt HW, Young YM (1982) Early Proterozoic climates and plate motions inferred from major element chemistry of lutites. Nature 299:715–717

Oyhantçabal P, Siegesmund S, Wemmer K, Presnyakov S, Layer P (2009) Geochronological constraints on the evolution of the

southern Dom Feliciano Belt (Uruguay). J Geol Soc London 166:1075–1084

Pankhurst RJ, Ramos A, Linares E (2003) Antiquity of the Río de la Plata craton in Tandilia, southern Buenos Aires province, Argentina. J S Am Earth Sci 16:5–13

Pankhurst RJ, Rapela CW, Fanning CM, Márquez M (2006) Gondwanide continental collision and the origin of Patagonia. Earth Sci Rev 76:235–257

Pazos PJ, Bettucci LS, Loureiro J (2008) The Neoproterozoic glacial record in the Rı′o de la Plata Craton: a critical reappraisal. In: Pankhurst RJ, Trouw RAJ, Brito Neves BB, De Wit MJ (eds) West Gondwana: Pre-Cenozoic Correlations across the South Atlantic Region. Geol Soc, London, Special Publ 294:343–364

Poiré DG (1987) Mineralogía y sedimentología de la Formación Sierras Bayas en el núcleo septentrional de las sierras homónimas, Partido de Olavarría, Provincia de Buenos Aires. PhD thesis, Universidad Nacional de La Plata, Argentina, 545pp

Poiré DG (1989) Stromatolites of the Sierras Bayas Group, Upper Proterozoic of Olavarría, Sierras Septentrionales, Argentina. Stromatolite Newsl XI:58–61

Poiré DG (1993) Estratigrafía del Precámbrico sedimentario de Olavaría, Sierras Bayas, Provincia de Buenos Aires, Argentina. XII Congreso Geológico Argentino y II Congreso de Exploración de Hidrocarburos Acta II:1–11

Poiré DG (2004) Sedimentary history of the Neoproterozoic of Olavarría, Tandilia System, Argentina: New evidence from their sedimentary sequences and unconformities—A "Snowball Earth" or a "Phantom" Glacial?; "1st Symposium on Neoproterozoic-Early Palaeozoic Events in SW-Gondwana", Extended Abstracts, IGCP Project 478, Second Meeting, Brazil, October 2004, 46–48

Poiré DG, Spalletti LA (2005) La cubierta sedimentaria precámbrica/palaeozoica inferior del Sistema de Tandilia. In: De Barrio RE, Etcheverry RO, Caballé MF, Llambías E (eds) Geología y Recursos Minerales de la provincial de Buenos Aires. Asociacion de Geología Argentina, La Plata, Relatorio del XVI Congreso Geológico Argentino 51–68

Poiré DG, Spalletti LA, Del Valle A (2003) The Cambrian-Ordovician siliciclastic platform of the Balcarce Formation (Tandilia System, Argentina): Facies, trace fossils, Palaeoenvironments and sequence stratigraphy. Geologica Acta 1:41–60

Poiré DG, Gómez Peral L, Bertolino S, Canalicchio JM (2005) Los Niveles con pirofilita de la Formación Villa Mónica, Precámbrico de Olavarría, Sistema de Tandilia, Argentina. XVI Congreso Geológico Argentino, Actas II:863–866

Poiré DG, Gaucher C, Germs G (2007) La superficie "Barker" y su importancia regional, Neoproterozoico del Cratón del Río de La Plata, Actas Sextas Jornadas Geológicas y Geofísicas Bonaerenses 36

Praekelt HE, Germs GJB, Kennedy JH (2008) A distinct unconformity in the Cango Caves Group of the Neoproterozoic to early Palaeozoic Saldania Belt in South Africa: its regional significance. S Afr J Geol 111:357–368

Rapalini AE, Poiré DG, Trindade R, Ficharte D (2008) Geochronologic and geodynamic implications of palaeomagnetic results from the Sierras Bayas Group, Rio de La Plata Craton (Argentina). VI South Amer Symp on Isotope Geology. Short Paper 1–3

Rapela CW, Pankhurst RJ, Casquet C, Baldo E, Saavedra J, Galindo C, Fanning CM (1998) The Pampean Orogeny of the southern proto-Andes: Cambrian continental collision in the Sierras de Cordoba. In: Pankhurst RJ, Rapela CW (eds) The Proto-andean Margin of Gondwana. Geol Soc London Spec Publ 142:181–217

Rapela CW, Pankhurst RJ, Fanning CM, Grecco LE (2003) Basement evolution of the Sierra del la Ventana Fold Belt: new evidence for Cambrian continental rifting along the southern margin of Gondwana. J Geol Soc London 160:613–628

Rapela CW, Pankhurst RJ, Casquet C, Fanning CM, Baldo EG, González-Casado JM, Galindo J, Dahlquist J (2007) The Río de la Plata craton and the assembly of SW Gondwana. Earth Sci Rev 83:49–82

Seilacher A, Congolani C, Varela R (2003) Ichnostratigraphic correlation of Early Palaeozoic sandstones in North Africa and Central Argentina. In: Salem MJ, Oun KM (eds) The geology of northwest Libya, pp 275–292

Spalletti LA, Del Valle A (1984) Las diamictitas del sector oriental de Tandilia: caracteres sedimentológicos y orígen. Rev de la Asoc Geol Arg 49:188–206

Spalletti LA, Poiré DG (2000) Secuencias silicoclásticas y carbonáticas del Precámbrico y Palaeozoico Inferior del Sistema de Tandilia, Argentina. Guía de Campo, II Congreso Latinoamericano de Sedimentología, 12-14.3.2000:1–39

Stanistreet IG, Kukla PA, Henry G (1991) Sedimentary basinal responses to a Late Precambrian Wilson Cycle: the Damara Orogen and Nama Foreland, Namibia. J Afr Earth Sci 13:141–156

Tankard AJ, Jackson MP, Erikson KA, Holiday DK, Hunter DR, Minter WEL (1982) Crustal Evolution of Southern Africa. Springer, New York, pp 1–523

Taylor SR, McLennan SM (1985) The Continental Crust: its Composition and Evolution. Blackwell, Oxford, pp 1–312

Theron JH (1972) The stratigraphy and sedimentation of the Bokkeveld Group. PhD thesis, University of Stellenbosch, 1–175

van Loon AJ (2000) The strangest 0.05% of the geological history. Earth Sci Rev 50:125–133

van Loon AJ (2008) Could 'Snowball Earth' have left thick glaciomarine deposits? Gondwana Res 14:73–81

Van Staden A, Naidoo T, Zimmermann U, Germs GJB (2006) Provenance analysis of selected clastic rocks in Neoproterozoic to lower Palaeozoic successions of southern Africa from the Gariep Belt and the Kango Inlier. S Afr J Geol 109:215–232

Van Staden A, Zimmermann U, Gutzmer J, Chemale F Jr, Germs GJB (2010) First regional correlation of Lower Palaeozoic successions from Argentina and South Africa using glacial diamictite deposits and its consequences for the regional geology. J Geol Soc London 167:217–220

von Eynatten H, Barceló-Vidal C, Pawlowsky-Glahn V (2003) Composition and discrimination of sandstones: a stochastic evaluation of different analytical methods. J Sed Res 73:47–57

Winchester JA, Floyd PA (1977) Geochemical discrimination of different magma series and their differentiation products using immobile elements. Chem Geol 20:325–343

Zack T, Kronz A, Foley SF, Rivers T (2002) Trace element abundances in rutiles from eclogites and associated garnet mica schists. Chem Geol 184:97–122

Zhang S, Jiang G, Junming Zhang J, Song B, Kennedy MJ, Christie-Blick N (2005) U-Pb sensitive high-resolution ion microprobe ages from the Doushantuo Formation in south China: constraints on late Neoproterozoic glaciations. Geology 33:473–476

Zimmermann U (2009) What was wrong with the Kalahari Craton? Rodinia: Supercontinents, Superplumes and Scotland—FERMOR Meeting. Geological Society of London, Programme and abstracts 59

Zimmermann U (2010) Detrital zircons the major tool or fool for provenance studies? 29th Nordic Geological Winter Meeting, Oslo, January 11–13:215

Zimmermann U, Bahlburg H (2003) Provenance analysis and tectonic setting of the Ordovician clastic deposits in the southern Puna Basin, NW Argentina. Sedimentology 50:1079–1104

Zimmermann U, Spalletti LA (2009) Provenance of the Lower Palaeozoic Balcarce Formation (Tandilia System, Buenos Aires

Province, Argentina): implications for palaeogeographic reconstructions of SW Gondwana. Sed Geol 219:7–23

Zimmermann U, Poiré DG, Gómez Peral L (2005) Provenance studies on neoproterozoic successions of the tandilia system (Buenos Aires Province, Argentina): preliminary data. XVI Congr Geol Arg Actas 4:6 pages CD ROM

Zimmermann U, Niemeyer H, Meffre S (2009a) Revealing the continental margin of Gondwana: the Ordovician arc of the Cordón de Lila (northern Chile). Int J Earth Sci. doi:10.1007/s00531-009-0483-8

Zimmermann U, Fourie P, Naidoo T, Van Staden A, Chemale F Jr, Nakamura E, Kobayashi K, Kosler J, Beukes NJ, Tait J (2009b) Unroofing the Kalahari craton: provenance data from Neoproterozoic to Palaeozoic Successions. Geochim et Cosmoch Actas 73(supp 1):A 1536